# Chapter 9

# ESTIMATION OF TISSUE BLOOD FLOW

*H. Frederick Bowman*

## 1. INTRODUCTION

Perfusion can be defined as the rate at which the quantity of blood in a given mass or volume of tissue is replenished at the level of the capillary network. The measurement of tissue blood flow (perfusion) is thus only a part, albeit a very significant part, of the larger task of blood flow measurement. For convenience this larger task can be divided into flow within the heart chambers, the arterial system, through the capillary network (perfusion), and back into the venous system.

The ability to measure perfusion in small volumes of tissue has been sought for many years, as this fundamental parameter holds the key to improved understanding of both normal and pathologic physiology as well as the diagnosis and subsequent management of many medical problems. The state of tissue perfusion is a primary factor in the local transport of (1) heat, the regulation of which is important for the clinical application of hyper- and hypothermia; (2) drugs, the delivery of which are critical throughout medical practice; and (3) oxygen and nutrients, which are crucial for effective surgical and medical management.

Indicator dilution methods have been developed and used widely for estimation of organ perfusion.[1–4] The general method follows from the Fick relation, in which the net transport of indicator into a region of interest is balanced by the transient buildup or removal of the indicator. Indicators that have been used for organ blood flow analysis include: injected radioactive and other diffusible gases,[5] locally generated hydrogen ion,[6] and injected or locally generated heat.[7] Trapped indicator methods, in which radiolabeled microspheres or aggregated albumin are distributed to a capillary bed in proportion to the local flow rate,[8] are currently receiving much attention. The subject of tissue blood flow measurement has recently been reviewed by Paradise and Fox.[4]

The purpose of this chapter is to review those thermal techniques used in estimation of tissue perfusion which are of historical significance,

*H. Frederick Bowman* • Department of Biomedical Engineering, Northeastern University, Boston, Massachusetts 02115; and Harvard–MIT Division of Health Sciences and Technology, Boston, Massachusetts 02138.

emphasizing those which are considered to be most promising. While many investigators have worked on the so-called heat clearance methods since the original work of Gibbs[9] some 50 years ago, their efforts have produced inconsistent, largely qualitative indices of perfusion rather than quantitative measurements of the important parameter. Attention is given here to the presentation and evaluation of techniques which derive from solution of the tissue energy balance known as the bioheat equation. Emphasis will be given to those works for which independent validation of tissue blood flow is provided. The advantages and limitations of the various techniques are noted.

It is acknowledged from the outset that, while much progress has been made, work in this field is incomplete and more development is required. Workers return to heat clearance methods because they are capable of meeting certain clinical requirements, where other techniques often have been less satisfactory. A clinical perfusion monitor must be safe for the patient, it must be applicable to any vascular bed, and it must be simple to operate. The results must be accurate and available immediately, and it must be possible to obtain repeated measurements. The attractiveness of the techniques based on thermal clearance is that, in principle, each of the above requirements is achievable.

Particular attention is given to the Thermal Diffusion Probe (TDP), a modular, microprocessor-based system developed over the past decade to facilitate bioheat transfer research by providing local real-time measurements of temperature, thermal properties, and blood perfusion.

## 2. THERMAL MODEL—TISSUE HEAT BALANCE

The temperature field in a homogeneous biological medium with isotropic thermal properties is described by a governing differential equation, which derives from a heat balance among the rate of change in internal energy, heat conduction, and convection into and out of the tissue medium, and local heat generation. The heat balance assumes that blood flow within the tissue is nondirectional at the capillary level; that is, the capillaries are assumed to be randomly oriented with respect to their arteriolar and venular connections. Convective heat exchange is assumed to occur only in this capillary system. It is further assumed that arteriovenous anastomoses play no role in heat transport. Local heat generation is also assumed to be a nondirectional property. With these assumptions, the balance between the heat transport mechanisms, in the specified order, is (cf. Chap. 7)

$$\rho c \frac{\partial T}{\partial t} = k\nabla^2 T + \rho_b c_b w_b (T_a - T_v) + q \tag{1}$$

As pointed out in Chap. 7, the microvascular contribution in tissue heat transfer is significant in that the equilibration of blood temperature with solid tissue takes place between the terminal arterial branches and the precapillary arterioles,[10] not in the capillaries as had originally been assumed.[11] Thus, except for heat transfer from the larger "thermally significant" vessels[12]

(which should be evaluated s
lature in a continuum formul
branches and smaller vessels.
Eq. (1) may be simplified to

$$\rho c \frac{\partial T}{\partial t} =$$

This simplified form is we
equation can be used to sol
sorts of conditions, althou
important in evaluating th
considerations which req
geometry, thermal property
of inhomogeneities in per
spatial and temporal chara
conditions (deep vs. superfi
temperature field, etc. Furt
can be best evaluated by a
by treating the tissue as a
vs. distributed tissue paran
by an analytical or by a n

Most applications of t
assumed that perfusion an
measurement volume), al
numerical solutions may

## 3. CLASSIFICATION

A wide variety of the
and thermal models, ha
perfusion. Others have
present are not fully de
techniques can be identi
ive vs. noninvasive; exte
region vs. coupled mu
planar, disk, etc.); and c

In Table 1, the most
techniques are identifie
techniques are identifie

Thermal clearance
tion and thus usually i
perfusion is estimated
forcing function, whic
temperature distributio
cal model, or considera
thermal property, whi

(which should be evaluated separately), the collective treatment of the vasculature in a continuum formulation is valid for blood vessels of terminal arterial branches and smaller vessels. Neglecting these "thermally significant" vessels, Eq. (1) may be simplified to

$$\rho c \frac{\partial T}{\partial t} = k\nabla^2 T - \rho_b c_b w_b (T - T_a) + q \tag{2}$$

This simplified form is well known as the bioheat transfer equation. This equation can be used to solve for tissue temperature distributions under all sorts of conditions, although sound thermal and analytical judgement is important in evaluating the relevance of each proposed model. Modeling considerations which require judgement include: an appropriate tissue geometry, thermal property values, the nature of the vasculature, the presence of inhomogeneities in perfusion, or in structure such as bone and air, the spatial and temporal characteristics of any absorbed thermal dose, boundary conditions (deep vs. superficial tissue), the expected accuracy of the predicted temperature field, etc. Further, it must be determined if the temperature field can be best evaluated by assuming the tissue to be finite or infinite in extent, by treating the tissue as a single or as multiple regions, by assuming lumped vs. distributed tissue parameters, or by solving the governing bioheat equation by an analytical or by a numerical technique.

Most applications of this equation for blood flow estimation have further assumed that perfusion and heating rates are uniform within the medium (or measurement volume), although this is not a necessary requirement when numerical solutions may be employed.

## 3. CLASSIFICATION OF PERFUSION ESTIMATION TECHNIQUES

A wide variety of thermal methods, employing differing probe techniques and thermal models, have been used to estimate the local value of tissue perfusion. Others have been suggested which hold promise but which at present are not fully developed. All thermally based perfusion estimation techniques can be identified by a six-dimensional classification scheme: invasive vs. noninvasive; external vs. self-heating; steady state vs. transient; single region vs. coupled multiregional; spherical vs. nonspherical (cylindrical, planar, disk, etc.); and qualitative vs. quantitative.

In Table 1, the most widely applied, thermally based perfusion estimation techniques are identified by this classification scheme. The originators of the techniques are identified by name and their published work is referenced.

Thermal clearance techniques all require an initial temperature perturbation and thus usually involve a transient measurement. Considered broadly, perfusion is estimated in one of two ways: determination of the value of a forcing function, which allows the best match of the experimentally observed temperature distribution (or rate of recovery) with that predicted by a theoretical model, or consideration of the contribution of perfusion to an intermediate thermal property, which is measured.

*TABLE 1*
*Classification of Thermally Based Perfusion Estimation Techniques*

| Method | Quantitative | Qualitative | Transient | Steady state | Geometry: Disk | Planar | Cylindrical | Spherical | Probe: Self-heating | External heating | Noninvasive | Invasive | Explicit solution for $w_b$ | Thermal model: Coupled BHTE with probe; conduction equation | Modified BHTE | Bioheat transfer equation (BHTE) |
|---|---|---|---|---|---|---|---|---|---|---|---|---|---|---|---|---|
| Muller-Schauenburg *et al.*[27] | | ● | ● | | ● | | | ● | | ● | ● | | ● | | ● | |
| Hensel[34,37] | | ● | ● | | ● | | | ● | | ● | ● | | ● | | ● | |
| Betz and Benzing[36] | | ● | ● | | ● | | | ● | | ● | ● | | ● | | ● | |
| Betz *et al.*[38] | | ● | ● | | ● | | | ● | | ● | ● | | ● | | ● | |
| Perl and Hirsch[24] | | | ● | ● | | | | ● | ● | | ● | | ● | | ● | |
| Tuttle and Sandler[15] | | ● | ● | | | | | | | ● | ● | | | | ● | |
| Cameron[16] | | ● | ● | | | | | | | ● | ● | | | | ● | |
| Mitchell *et al.*[20] | | ● | ● | | | | ● | | | ● | ● | | | | | ● |
| Eberhart *et al.*[18] | | ● | ● | | ● | | | | | ● | ● | | | | | ● |
| Hernandez *et al.*[19] | | ● | ● | | | ● | | | | ● | ● | | | | | ● |
| Shitzer[22] | | ● | ● | | | ● | | | | ● | ● | | | | | ● |
| Bowman *et al.*[28] | ● | | ● | ● | | | | ● | ● | | ● | ● | ● | ● | | |
| Balasubramaniam and Bowman[41] | ● | | ● | ● | | | | ● | ● | | ● | ● | ● | ● | | |
| Woods and Bowman[48] | ● | | ● | ● | | | | ● | ● | | ● | ● | ● | ● | | |
| Valvano and Bowman[17] | ● | | ● | ● | | | | ● | ● | | ● | ● | ● | ● | | |
| Chen and Holmes[29] | | ● | ● | | | | | ● | ● | | ● | | | | ● | |
| Johnson *et al.*[25] | | ● | ● | | | | | ● | ● | | ● | | | | | |
| Patera *et al.*[30] | ● | | ● | | | ● | | ● | ● | ● | | ● | | ● | | ● |
| Bowman and Walsh[32] | ● | | ● | | | ● | | ● | ● | ● | | ● | | ● | | |
| Walsh and Bowman[33] | ● | | ● | | | ● | | ● | ● | ● | | ● | | ● | | |
| Eden and Bowman[31] | ● | | ● | | | | ● | | ● | | ● | ● | | ● | | |

In the former approach the initial temperature perturbation may be established by a number of methods. The so-called "passive probe" methods utilize external heating or cooling of the tissue specimen by: injecting a cold bolus of fluid in the arterial supply[15–17]; altering the incoming blood flow rate,[18] blood temperature,[19] surface temperature,[20] or surface heat flux[21]; or a response to exercise which is modeled as a combined alteration of flow rate and metabolic heat generation rate.[22] A number of heated probe techniques have also been developed.[23–25] Regardless of how the temperature perturbation is established in the tissue, the subsequent experimentally measured $T(r, t)$ is then compared with a theoretical $T(r, t)$ predicted by a solution of a thermal model with appropriate initial and boundary conditions. The thermal model may be based on the full bioheat equation, a simplification of this equation, or either of these, coupled with the governing conduction

equation in the sensing pr
an inverse problem, in tha
temperature, $T$. The most
probe surface or volume a
thermal perturbation, wh
alter the tissue temperatur
of the theoretical model
systematically varying the
until the theoretical–expe
least-squares sense. When
butions match over the ap
that the correct perfusion
mental protocols and the n
rate may be determined s

Our ability to quant
promising, particularly w
and time.[26] The second a
from intermediate therma
is much more promising,

We start our discussi
measurement of thermal
originally introduced by
Benzing, and Muller-Sch
in Europe today. This r
conductivity, which has
general technique will b
this approach is describe
heated thermistor probe
term, also based on me
thermal diffusivity. A de
verification is given in S
unexploited, variants of
methods have recently b
of Chen and Holmes,[29]
and Eden and Bowman
Walsh.[32,33]

## 4. METHODS OF HE
## MÜLLER-SCHAUE

The principle of th
perature difference whi
probe. Mathematically t
law of heat conduction,

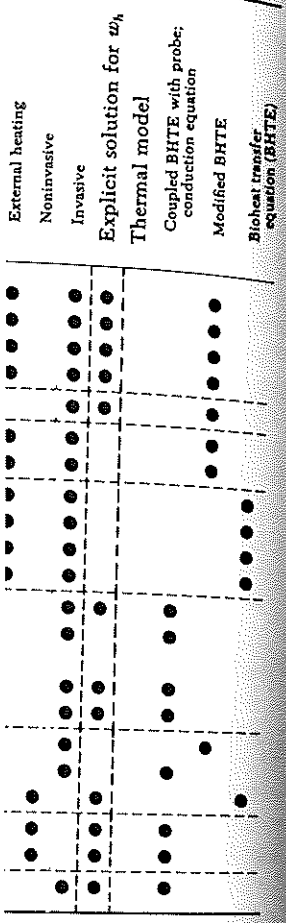


perturbation may be
ssive probe" methods
n by: injecting a cold
incoming blood flow
r surface heat flux[21];
ıed alteration of flow
of heated probe tech-
how the temperature
uent experimentally
$T(r, t)$ predicted by a
boundary conditions.
ıtion, a simplification
overning conduction

equation in the sensing probe. This estimation problem may be classified as an inverse problem, in that $w_b$ is in general an implicit function of the tissue temperature, $T$. The most commonly employed technique is to measure the probe surface or volume averaged temperature field in response to the specific thermal perturbation, where it is assumed that the sensing probe does not alter the tissue temperature field. The best match of the appropriate solution of the theoretical model to the measured temperature is then produced by systematically varying the values of the perfusion rate in the analytical solution until the theoretical–experimental temperature difference is minimized in a least-squares sense. When the experimental and theoretical temperature distributions match over the appropriate period of thermal recovery, it is concluded that the correct perfusion rate has been determined. Depending on the experimental protocols and the nature of the thermal model, tissue metabolic heating rate may be determined simultaneously.[19,22]

Our ability to quantify perfusion with this first approach is not very promising, particularly when the tissue is not uniformly perfused in space and time.[26] The second approach of direct or indirect extraction of perfusion from intermediate thermal property (conductivity/diffusivity) measurements is much more promising, and thus is the focus of this chapter.

We start our discussion of the perfusion estimation techniques based on measurement of thermal properties with the qualitative, indirect approach originally introduced by Gibbs[9] and subsequently improved by Hensel, Betz, Benzing, and Muller-Schauenburg,[27] a technique which is widely employed in Europe today. This method embodies the concept of effective thermal conductivity, which has been recently developed to a higher degree. This general technique will be discussed in some detail. Further development of this approach is described by Bowman *et al.*,[28] whose analysis of the self-heated thermistor probe has led to explicit solutions for the tissue perfusion term, also based on measurements of effective thermal conductivity and thermal diffusivity. A detailed exposition of Bowman's approaches and their verification is given in Sections 5–13. Other promising, though still largely unexploited, variants of the intermediate thermal property measurement methods have recently been proposed. These include the pulse-decay method of Chen and Holmes,[29] the periodic excitation methods of Patera *et al.*[30] and Eden and Bowman,[31] and the noninvasive method of Bowman and Walsh.[32,33]

## 4. *METHODS OF HENSEL–BETZ–BENZING AND MÜLLER-SCHAUENBURG*

The principle of this method is based on the measurement of the temperature difference which is established between a heated and an unheated probe. Mathematically the analysis is performed in accordance with Fourier's law of heat conduction,

$$q = -Ak\Delta T/\Delta L \tag{3}$$

The reciprocal temperature difference between the heated and unheated tissue sites is proportional to the thermal conductivity when the applied power is constant. When used in living tissue, the augmentation of heat dissipation from the heated probe due to the perfusion is observed as a decreased temperature difference, reflecting an increase (perfusion dependent) in effective or apparent thermal conductivity.

Hensel's measurements[34] were made with needle-shaped probes containing a heated thermojunction in their tips or shafts, and with linear probes made from thin, flexible, copper-constantan wires that were freely pulled through the tissue of interest. Such probes have been used to measure blood flow in muscle[35] and in myocardium.[36] A typical probe configuration for this approach is shown in Fig. 1. Hensel also developed a disk-shaped device that has been placed on the tissue surface for superficial measurements of blood flow in skin and brain.[37]

While probe configurations have taken many forms, the operating principle has remained the same. Local blood flow measurements are carried out in one of two modes of operation: (1) "slug heating," in which a thermistor is heated for a very short time and the temperature change is subsequently recorded; or (2) the sudden introduction of heat to the heated probe (by switching "on and off" a heating coil surrounding a micro-thermistor) and recording the subsequent tissue temperature history.

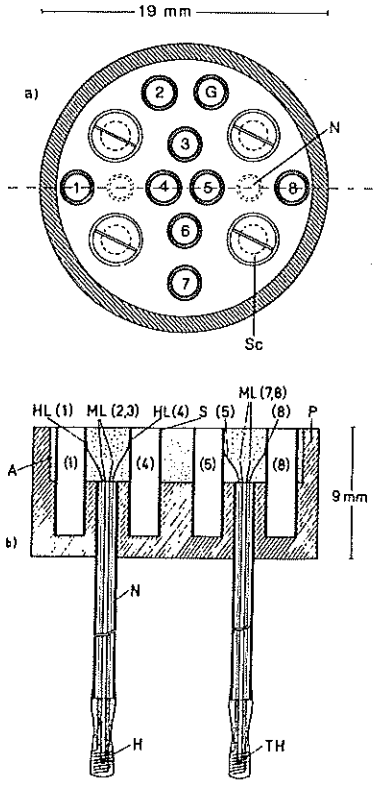


*FIGURE 1*

Sectional drawing of a heat clearance device for measurement of local blood flow in the interior of the brain. (a) Transverse sectional view through socket and needles (N); (b) longitudinal section. The needles are implanted through narrow burr holes in the skull. The socket is fixed with 4 screws (Sc) in the bone of the skull. It is made of Plexiglas (P). Into the socket 8 tubes made of silver (S) are cast with Araldit (A). A plug with 8 pins, which fit into the silver tubes, connects the measuring device with the recording instrument. The plug is not seen in this drawing. Leads for heating the needle tip (HL) and measuring leads (ML) for temperature are placed within the needles (0.7–1 mm diam). Diameter of the insulated copper placed within the needle is 0.05 mm. In the Araldit-covered tip of the needle the thermistors (TH) with surrounding heating coils (H) are soldered to the leads. The measuring leads and the heating leads are soldered to the silver tubes 1–8 in the socket in such a way that every thermistor can be heated. G = ground. (Reproduced from Ref. 27, with permission.)

The slug heating approac
1) where the temperature pert
probe. Betz *et al.*[38] show
temperature curves derived fr
bed by slug heating in accor

Betz[38] defines $U_{slug}$ as the t
which is a function of locat
coefficient $\lambda \equiv [(\rho c)_{tissue}/(\rho c$
unperfused tissue, respective
vessels supplying the tested
zero perfusion. The temper
thus, as a method to quantit
assessment of flow from api
the original work for furthe

The second method of
tively turned on and off is
perfusion in various tissues
Fig. 2. The cooling curve

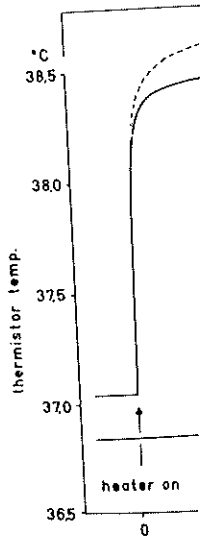


*FIGURE 2*

Time course of thermistor te
temperature. Solid line: Meas
change after turning on the h
the living animal. The refere
of the basic tissue temperatu
from these curves. (Reproduc

The slug heating approach is similar to the passive probe methods (Table 1) where the temperature perturbation is introduced with the invasive heated probe. Betz *et al.*[38] show that perfusion can be estimated from time–temperature curves derived from both perfused and unperfused tissue perturbed by slug heating in accordance with

$$\frac{U_{\text{slug},\phi}}{U_{\text{slug},0}} = \exp\left(-\frac{\phi t}{\lambda}\right) \tag{4}$$

Betz[38] defines $U_{\text{slug}}$ as the temperature field increment of the heated tissue which is a function of location, time, perfusion $\phi$, ($ml_{blood}/ml_{tissue}$ min) and coefficient $\lambda \equiv [(\rho c)_{\text{tissue}}/(\rho c)_{\text{blood}}]$. Subscripts $\phi$ and 0 refer to perfused and unperfused tissue, respectively. This technique requires an occlusion of blood vessels supplying the tested region to estimate the temperature history for zero perfusion. The temperature history for perfused tissue is uncalibrated; thus, as a method to quantitate flow, the technique requires an independent assessment of flow from application to application. The reader is referred to the original work for further details on this method.[35]

The second method of Betz *et al.*[27] in which the heated probe is alternatively turned on and off is used routinely to evaluate relative levels of blood perfusion in various tissues. A typical time–temperature profile is shown in Fig. 2. The cooling curve (heater off) is the inverse mirror image of the

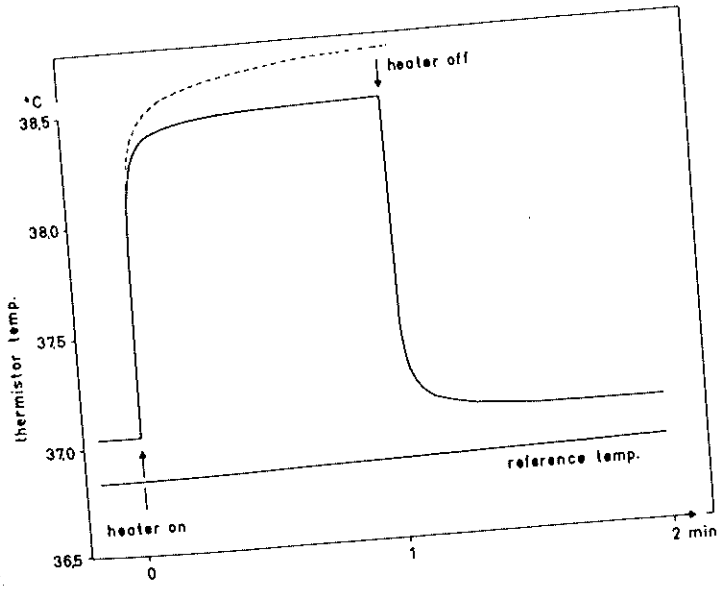


***FIGURE 2***
Time course of thermistor temperature (brain). Turning on the heater causes an increase in temperature. Solid line: Measurement in a living animal. The dashed line gives the temperature change after turning on the heater in a dead animal at the same initial tissue temperature as in the living animal. The reference temperature is not parallel with the abscissa, so that the trend of the basic tissue temperature has to be taken into account when the blood flow is evaluated from these curves. (Reproduced from Ref. 27, with permission.)

warming curve (heater on). Their data reduction protocol is as follows. The temperature difference between the tissue site (temperature sensing probe) and the reference temperature (tissue baseline) is determined as

$$U(t) = T_s(t) - T_{\text{ref}}(t) \tag{5}$$

The rate of change of the temperature difference at the tissue sensing site then forms the basis of their evaluation:

$$\frac{dU(t)}{dt} = |\dot{U}_{\text{on}}| = |\dot{U}_{\text{off}}| = \tan \alpha \tag{6}$$

The slope, $\tan \alpha$, is graphically determined at different times, typically between 15 and 45 s. Perfusion is estimated as shown in Fig. 3 from the following expression:

$$\frac{(\tan \alpha)_{\text{flow}}}{(\tan \alpha)_{\text{no flow}}} = \exp\left(-\frac{w_b t}{\lambda}\right) \tag{7}$$

where $\phi$ is defined as $w_b$ and the partition coefficient $\lambda$ is defined as $\rho_t c_t / \rho_b c_b$.

As shown in Fig. 3b, a linear least-squares curve fit yields the slope $(\phi/\lambda)10^{\log e}$. Blood flow, $w_b$, is then calculated by multiplying the slope by $\lambda/0.434$. The value of $\lambda$ is determined from the "death curve" and the specific heat of blood.[27]

Perl and Hirsch[24] provided a more detailed analysis of the simple washout model based on a simplification of Eq. (2) where the conduction term is neglected. They also included a comparison with an independent perfusion rate measurement technique. Their method was apparently prompted by an empirical technique reported by Stow and Scheive.[23] The probe employed in this study consisted of a hypodermic needle (No. 20) with a thermistor placed near the tip; along the outside of the needle was mounted a hairpin loop of fine insulated wire which served as a heat source. With the needle inserted into the renal cortex, four transient temperature responses were produced and recorded. With heater power regulated to elevate needle temperature by 0.5–1°C, blood flow was suddenly stopped by simultaneously clamping off the renal artery and vein. Eight seconds later the clamps were released and the temperature recovery was recorded. Heater power was then turned off, and 2–3 min later the clamp–release maneuver was repeated. Noting that a sudden change in the rate of perfusion would elicit a discontinuous change in the temporal derivative of temperature, which would serve to approximate conducted heat flux, Perl and Hirsch produced a relation between blood perfusion rate and the rate of change of internal energy:

$$w_b(T_a - T) = \lambda\left[\left(\frac{dT}{dt}\right)_1 - \left(\frac{dT}{dt}\right)_2\right] \tag{8}$$

Subscripts 1 and 2 denote conditions prior to and immediately following

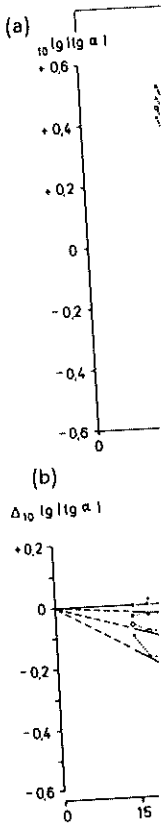


*FIGURE 3*
Evaluation of local blood flow of heat clearance in nonperfu measurement in gelatin. The l similar to that of muscle tissu different slopes, depending on e.g., in hypoxia (9% $O_2$). Lo produced by occlusion of a c nonperfusion curve. By defin right scale gives the flow val λ (tissue/blood) in the myoca to be multiplied by 0.9. (Rep

occlusion, respectively an elevated tissue temp is sufficiently small th relation for the heated (8). Defining $u$, the tem the authors related th measured prior to occl

$w_b$

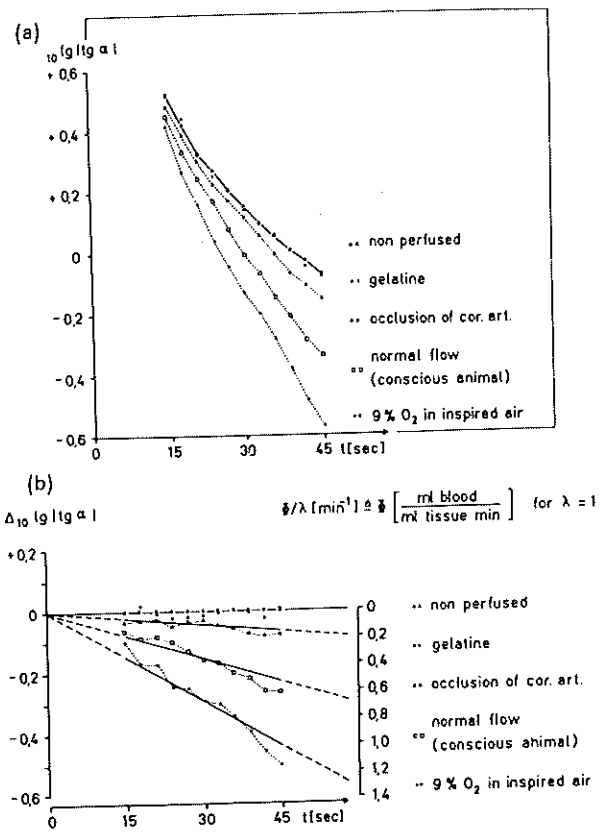


*FIGURE 3*
Evaluation of local blood flow in the myocardium of the left ventricle in a dog and comparison of heat clearance in nonperfused heart (after the death of the animal) with a heat clearance measurement in gelatin. The heat conductivity of gelatin ($K = 12.5 \times 10^{-1}$ cal cm$^{-1}$ s$^{-1}$ °C$^{-1}$) is similar to that of muscle tissue. (a) The logarithm of the slope of heat clearance curves shows different slopes, depending on the blood flow. Steep slopes are obtained in high flow conditions, e.g., in hypoxia (9% $O_2$). Low flow values were obtained within infarcted areas which were produced by occlusion of a coronary artery. (b) Differences of (a) obtained by subtracting the nonperfusion curve. By definition the nonperfusion curve now corresponds to the $x$ axis. The right scale gives the flow values in ml blood/ml tissue min. Since the heat partition coefficient λ (tissue/blood) in the myocardium is 0.9 instead of 1 the flow values obtained (right scale) have to be multiplied by 0.9. (Reproduced from Ref. 27, with permission.)

occlusion, respectively. With introduction of heat into the tissue to produce an elevated tissue temperature, and assuming that the temperature elevation is sufficiently small that local perfusion is unaltered, the authors derived a relation for the heated condition exactly as for the unheated condition, Eq. (8). Defining $u$, the temperature difference for heater on–heater off conditions, the authors related the local perfusion $w_b$ to the temperature difference measured prior to occlusion and immediately following occlusion:

$$w_b = \lambda \left[ \left( \frac{du}{dt} \right)_2 - \left( \frac{du}{dt} \right)_1 \right] [u(t) - u_a(t)]^{-1} \tag{9}$$

Perl and Hirsch also modeled the discrete heat-sink effect of large blood vessels in the vicinity of the temperature probe. The authors compared the perfusion estimate, Eq. (9), with an independent estimation of renal flow by *para*-aminohippurate (PAH) clearance and found that it underestimated the PAH clearance result by a factor of 2. The transient heat clearance method provided reproducible results, but was subject to errors due to tissue displacement, needle heat conduction, and the presence of large vessels. From the discrete heat-sink effect of large blood vessels, Perl and Hirsch calculated a relation between the center-to-center distance between the large vessels and their diameter that agreed with the dimensions and spacing of afferent renal arterioles.[39] The importance of Perl and Hirsch's work lies not only in its originality, but also in the demonstrated ability to estimate the effects of large vessels in the proximity of the temperature probe on the prediction of the tissue perfusion rate. Difficulties in providing a total occlusion of the blood supply and other errors inherent in approximating heat diffusion by the clamping maneuvers may limit the successful extension of this method.

## 5. MODELING FOR THERMAL PROPERTY AND PERFUSION MEASUREMENTS

Bowman, Balasubramanian, and Woods[28] developed a method for estimating perfusion rate, following a suggestion by Chato.[40] The method was first applied for the measurement of thermal conductivity,[41] and then extended to the measurement of effective thermal conductivity.[28] It differs from the previously considered effective thermal conductivity techniques, since $w_b$ is calculated explicitly. Refinements of this original technique have been made recently, which may qualify the technique for the rigorous clinical requirements listed previously. In all of the methods of Bowman *et al.* discussed herein, one starts with a small, self-heated thermal probe.

The essence of the thermal probe is an electrically resistive thermistor bead mounted at the tip of either an insulating needle or catheter. The ellipsoidal thermistor bead (modeled as a sphere) is first used passively to sense the temperature of the tissue and is then heated. Electrical energy is dissipated in the bead at a rate sufficient to maintain the temperature of the bead at some predetermined fixed increment above the initial equilibrium temperature of the bead and the surrounding tissue $T_0$. The electrical power required to maintain this temperature increment depends upon the heat transfer characteristics of the surrounding tissue. The presence of blood flow augments heat transfer both in the steady and nonsteady states. As is shown schematically in Fig. 4, the presence of flow requires more steady state electrical power to maintain a given temperature step. The concept of "effective" thermal conductivity, $k_{\text{eff}}$, lumps together the intrinsic conductivity, $k_m$, of the tissue with the contribution of blood flow to the steady state heat transfer. The concept of "effective" thermal diffusivity, $\alpha_{\text{eff}}$, lumps together the intrinsic diffusivity, $\alpha_m$, of the tissue with the contribution of blood flow to the transient heat transfer. The presence of perfusion increases the temporal

*FIGURE 4*
Schematic of idealized the
deposition history in unperfu
fused (effective) media. $V$
$R(T, t)$: thermistor resistance
to medium; $\Delta T_b$: thermistor
vation; $d$: temperature decay

response of tissue to a
steady state condition.

## 6. ANALYTICAL M

Accurate measure
thermally based techn
interactions between t
measured. The tempe
tissue is described by t
here as

$$\nabla^2$$

where the subscripts
blood, respectively;
and $\alpha_m$ is the therma
spherical thermistor
time-dependent, sph
rounding the bead is

$$\frac{1}{r^2}\frac{\partial}{\partial r}\left(r^2\right.$$

where $V_m \equiv T_m - T$
the bead itself is a r
electrical power wit
bead.

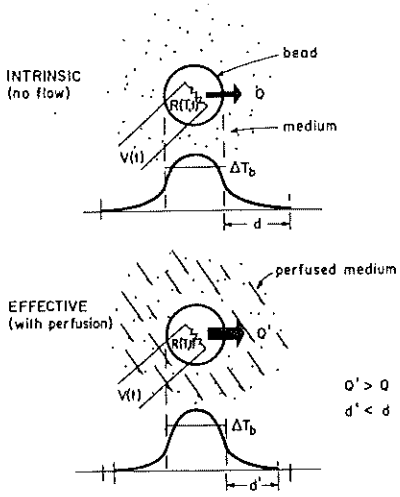


*FIGURE 4*
Schematic of idealized thermistor-based power deposition history in unperfused (intrinsic) and perfused (effective) media. $V(t)$: applied voltage; $R(T, t)$: thermistor resistance; $Q$: power delivered to medium; $\Delta T_b$: thermistor mean temperature elevation; $d$: temperature decay distance.

response of tissue to a thermal perturbation, and thus the rate of return to a steady state condition.

## 6. ANALYTICAL MODEL

Accurate measurement of thermal properties and perfusion using this thermally based technique requires a model which accounts for the thermal interactions between the measurement device and the medium (tissue) being measured. The temperature field in a continuous, homogeneous, perfused tissue is described by the bioheat equation [Eq. (2)] developed earlier, written here as

$$\nabla^2 T_m + \frac{q_m}{k_m} - \frac{\rho_b c_b w_b}{k_m}(T_m - T_a) = \frac{1}{\alpha_m}\frac{\partial T_m}{\partial t} \tag{10}$$

where the subscripts $m$ and $a$ refer to the tissue medium and the arterial blood, respectively; $w_b$ is the local perfusion, $c_b$ is heat capacity of blood, and $\alpha_m$ is the thermal diffusivity of the tissue defined as $\alpha_m = k_m/\rho c$. For a spherical thermistor bead of radius $a$ immersed in a tissue medium $m$, the time-dependent, spherically symmetric temperature field in the medium surrounding the bead is given by

$$\frac{1}{r^2}\frac{\partial}{\partial r}\left(r^2\frac{\partial V_m}{\partial r}\right) + \frac{q_m}{k_m} - \frac{\rho_b c_b w_b}{k_m}(T_m - T_a) = \frac{1}{\alpha_m}\left(\frac{\partial T_m}{\partial t}\right) \tag{11}$$

where $V_m \equiv T_m - T_0$, and $T_0$ is the initial temperature of the tissue. Since the bead itself is a medium of finite thermal conductivity, the dissipation of electrical power within the bead results in a temperature distribution in the bead.

If the bead, which in reality is a composite, prolate spheroid, is taken as a sphere of radius $a$, the temperature field generated by the thermal probe within perfused tissue is described by the coupled tissue–thermal probe equations in spherical coordinates, $r$, as

$$\frac{1}{r^2}\frac{\partial}{\partial r}\left(r^2\frac{\partial V_p}{\partial r}\right)+\frac{\Gamma+\beta f(t)}{k_p}=\frac{1}{\alpha_p}\left(\frac{\partial V_p}{\partial t}\right) \qquad r \leqslant a \tag{12}$$

$$\frac{1}{r^2}\frac{\partial}{\partial r}\left(r^2\frac{\partial V_m}{\partial r}\right)+\frac{\Psi-\rho_b c_b w_b V_m}{k_m}=\frac{1}{\alpha_m}\frac{\partial V_m}{\partial t} \qquad r \geqslant a \tag{13}$$

where $V_p = T_p - T_0$ is the reduced temperature field within the probe (bead), $\Gamma + \beta f(t)$ is the time-dependent volumetric heat generation rate (assumed uniform throughout the bead) required to maintain the bead at a constant temperature increment above the tissue baseline temperature, $T_0$, and

$$\Psi = q_m + \rho_b w_b c_b (T_a - T_0) \tag{14}$$

This coupled set of second-order, partial differential equations represents the general governing equations for the probe and tissue and requires two initial and four boundary conditions for solution. The four boundary conditions assumed are symmetry at the origin, continuity of flux and temperature at the probe–tissue interface, and negligible temperature perturbation at large distances from the probe. Initially both the probe and tissue are at the tissue base-line temperature:

$$V_m = 0 \qquad \text{at } t = 0 \tag{15}$$

$$V_p = 0 \qquad \text{at } t = 0 \tag{16}$$

$$\frac{\partial V_p}{\partial r} = 0 \qquad \text{at } r = 0 \tag{17}$$

$$-k_p\frac{\partial V_p}{\partial r} = -k_m\frac{\partial V_m}{\partial r} \qquad \text{at } r = a \tag{18}$$

$$V_p = V_m \qquad \text{at } r = a \tag{19}$$

$$V_m \to 0 \qquad \text{as } r \to \infty \tag{20}$$

## 7. SOLUTION METHODS

### 7.1. Partial Solutions of the Governing Equations

The original technique for measurement of thermal conductivity and diffusivity is based on the solution of the time-dependent, coupled equations

without consideration of
This is basically the solut
bolic terms set equal to z

and $f(t)$ set equal to $t^{-1/2}$
giving effective thermal
±1%. "Sample" volumes
achieved by varying the
one minute. Sample volu
by the heated probe witl
separate determination
conductivity, $k_p$. These
known materials such as

Expanding this tecl
including metabolic hea
ment of the modified m
perfusion from *in vivo* m
model allowed the isola
intrinsic tissue thermal
thermal conductivity in
Eqs. (12) and (13) redu

$$\frac{1}{r}$$

*FIGURE 5*
Determination of the effecti
ized spherical thermistor bea
conductivity. See Ref. 44 f
from Ref. 28, with permissi

without consideration of metabolic heat generation or tissue perfusion.[42] This is basically the solution of Eqs. (12)–(20) with the perfusion and metabolic terms set equal to zero, or

$$\frac{\Psi - \rho_b c_b w_b V_m}{k_m} = 0 \tag{21}$$

and $f(t)$ set equal to $t^{-1/2}$. The technique can be applied *in vitro* and *in vivo*, giving effective thermal conductivity values with accuracies of the order of ±1%. "Sample" volumes of less than 0.05 to greater than 1.5 ml are readily achieved by varying the measurement time from as short as 5 s to as long as one minute. Sample volumes are defined as the volume thermally perturbed by the heated probe within the measurement period. The method requires a separate determination of the effective probe radius, $a$, and probe thermal conductivity, $k_p$. These calibrations are made, based on reference values of known materials such as agar gel, glycerol, and castor oil, as shown in Fig. 5.

Expanding this technique to solve the coupled steady state equations, including metabolic heat generation and tissue perfusion, led to the development of the modified method of Bowman and Balasubramaniam to quantify perfusion from *in vivo* measurements of thermal conductivity.[28] The thermal model allowed the isolation of the perfusion term, $w_b$, from measurements of intrinsic tissue thermal conductivity in the absence of flow and effective thermal conductivity in the presence of flow. For the steady state problem Eqs. (12) and (13) reduce to, respectively,

$$\frac{1}{r^2}\frac{\partial}{\partial r}\left(r^2 \frac{\partial V_p}{\partial r}\right) + \frac{\Gamma}{k_p} = 0 \qquad r \leqslant a \tag{22}$$

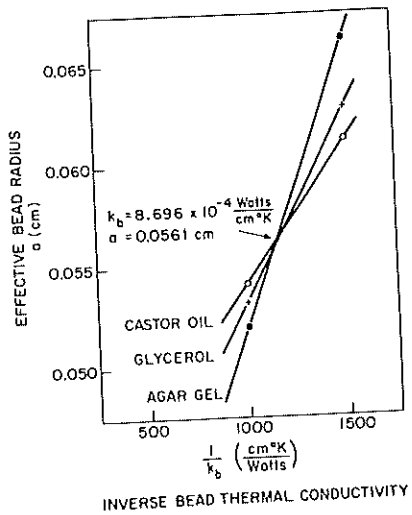


*FIGURE 5*
Determination of the effective radius, $a$ of an idealized spherical thermistor bead; $k_b$ is the bead thermal conductivity. See Ref. 44 for details. (Reproduced from Ref. 28, with permission.)

and

$$\frac{1}{r^2}\frac{\partial}{\partial r}\left(r^2\frac{\partial V_m}{\partial r}\right)+\frac{\Psi-\rho_b c_b w_b V_m}{k_m}=0 \qquad r \geqslant a \tag{23}$$

Solving the coupled steady-state diffusion equations (22) and (23) together with the boundary conditions of symmetry at $r = 0$, continuity of temperature and heat flux at $r = a$ and zero temperature rise as $r \to \infty$, the resulting temperature distributions within the probe and surrounding tissue are, respectively,

$$V_p(r) = T_p(r) - T_0 = \frac{\Gamma a^2}{6k_p}\left(1-\frac{r^2}{a^2}\right)+\frac{\Psi}{\rho_b c_b w_b}+\frac{\Gamma a}{3k_m} \times\left[\frac{1}{(\rho_b c_b w_b/k_m)^{1/2}+1/a}\right] \tag{24}$$

$$V_m(r) = T_m(r) - T_0 = \frac{\Gamma a^2}{3k_m}\frac{\exp\left[\rho_b c_b w_b/k_m(a-r)\right]}{(\rho_b c_b w_b/k_m)^{1/2}+1/a}+\frac{\Psi}{\rho_b c_b w_b} \tag{25}$$

The property of the thermistor bead actually measured is its electrical resistance rather than its temperature, that is, the electrical resistance averaged over the volume of the bead. Since the bead resistivity is a direct function of temperature, its electrical resistance, $R$, is an indirect measurement of the volume averaged temperature increment $\bar{V}_p$, where

$$\bar{V}_p = \frac{3}{4\pi a^3}\int_0^a 4\pi r^2 V_p(r)\,dr \equiv \Delta T_p \tag{26}$$

In practice, $\Delta T_p$ is calculated as the difference of the spatially averaged bead temperature and the initial tissue temperature, as

$$\Delta T_p = \frac{\Gamma a^2}{3k_p}\left\{\frac{k_p}{k_m}\left[\left(\frac{\rho_b c_b w_b a^2}{k_m}\right)^{1/2}+1\right]^{-1}+0.2\right\}+\frac{\Psi}{\rho_b c_b w_b} \tag{27}$$

When the probe is unheated, $\Gamma = 0$ and the bead assumes the initial tissue temperature:

$$\Delta T_p = \frac{\Psi}{\rho_b c_b w_b} = 0 \tag{28a}$$

or from Eq. (14),

$$T_p = T_0 = T_a + \frac{q}{\rho_b c_b w_b} \tag{28b}$$

which shows that the r
initial or base-line temp
$\Delta T_p$ is derived from Eq

$$\Delta T_p = \frac{\Gamma}{3}$$

Bowman *et al.*[28] show
the intrinsic tissue cond
lumped together to forr
above. For this situatio

Combining Eqs. (29)
explicitly as

This is the fundamenta
and also for the transi
of the effective bead ra
situation derives from
phenomenon with ur
conductivity are in pc

which shows that the
perfusion and intrinsi
of the probe bead. Th
one must know the e
the effective thermal
the intrinsic thermal c
thermal conductivity
mental parameters in

where $R$ is the resis
steady-state voltage
increment above the
tion of the bead's ra
substantial source of

which shows that the metabolic heat generation, $q$, serves to establish the initial or base-line temperature. When $T_0$ is defined according to Eq. (28b), $\Delta T_p$ is derived from Eq. (27) as

$$\Delta T_p = \frac{\Gamma a^2}{3k_p}\left\{\frac{k_p}{k_m}\left[\left(\frac{\rho_b c_b w_b a^2}{k_m}\right)^{1/2} + 1\right]^{-1} + 0.2\right\} \tag{29}$$

Bowman *et al.*[28] show that $\Delta T_p$ can be rederived for the situation in which the intrinsic tissue conductivity and convective heat flux due to perfusion are lumped together to form an effective thermal conductivity, $k_{\text{eff}}$, as described above. For this situation, Eq. (29) reduces to

$$\Delta T_p = \frac{\Gamma a^2}{3k_p}\left(\frac{k_p}{k_{\text{eff}}} + 0.2\right) \tag{30}$$

Combining Eqs. (29) and (30), the perfusion term may be obtained explicitly as

$$w_b = \left(\frac{k_{\text{eff}}}{k_m} - 1\right)^2 \frac{k_m}{\rho_b c_b a^2} \tag{31}$$

This is the fundamental relation for the steady state thermal property method, and also for the transient method to be described later. Note that the square of the effective bead radius, $a^2$, appears in the denominator of Eq. (31). This situation derives from the fact that perfusion is a convective augmentation phenomenon with units of power/unit length squared, whereas units of conductivity are in power/unit length. Equation (31) can be rearranged as

$$k_{\text{eff}} = k_m\left[\left(\frac{\rho_b c_b w_b a^2}{k_m}\right)^{1/2} + 1\right] \tag{32}$$

which shows that the effective thermal conductivity of tissue, with a given perfusion and intrinsic conductivity, $k_m$, is a linear function of the radius, $a$, of the probe bead. Thus, in order to quantify perfusion using this approach, one must know the effective dimensions of the probe bead used to measure the effective thermal conductivity of the tissue. As discussed in Ref. 28, both the intrinsic thermal conductivity in the absence of perfusion and the effective thermal conductivity in the presence of perfusion are calculated from experimental parameters in accordance with the following expression:

$$k_m = \left(\frac{4\pi a \Delta T_p R}{V_{ss}^2} - \frac{0.2}{k_p}\right)^{-1} \tag{33}$$

where $R$ is the resistance of the heated bead and $V_{ss}^2$ is the square of the steady-state voltage required to maintain the bead at the predetermined fixed increment above the initial tissue temperature. The experimental determination of the bead's radius, $a$, discussed in an earlier paper[41] may introduce a substantial source of error in practice, unless care is taken in the measurement.

Generally, a measurement under no blood flow conditions is necessary to obtain the intrinsic tissue conductivity, $k_m$. However, it is theoretically possible to determine the intrinsic tissue conductivity by measurements using two probes of different bead size, located sufficiently close together that they are exposed to the same level of perfusion. Eliminating $w_b$ [Eq. (31)], we obtain

$$\left(\frac{k_{\text{eff}\,1}}{k_m} - 1\right)^2 \frac{1}{a_1^2} = \left(\frac{k_{\text{eff}\,2}}{k_m} - 1\right)^2 \frac{1}{a_2^2} \tag{34}$$

where $k_m$ is the only unknown quantity.

Considerable effort has been expended in investigating the accuracy of perfusion measured by Eq. (31). The isolated canine hind limb, isolated canine gracilis muscle, and isolated rat liver have been used in controlled perfusion model systems. Bowman *et al.*[28] first correlated the total blood flow rate of an isolated canine hind limb with the square of the bracketed conductivity term, $[(k_{\text{eff}}/k_m) - 1]^2$. A linear relation was obtained over a tenfold range of blood flow values. No direct experimental–analytical perfusion comparison was made, owing to the difficulty of quantifying the fraction of total flow through the bone, skeletal muscle, and skin. However, the linear relationship found between total limb flow and $[(k_{\text{eff}}/k_m) - 1]^2$ suggested the analytical model was valid, and thus seemed to justify the use of the bioheat equation.

Typical early results of this method in model experiments are presented in Fig. 6 for two situations: the probe positioned (a) "far" from a large blood vessel, and (b) "close" to a large blood vessel. The data are presented as probe power dissipation vs. the inverse of the square root of time, $t^{-1/2}$. Recall that this first method is based on a steady state solution of the governing equations, (12)–(20). However, this method derives from the prior transient conductivity measurement technique of Balasubramaniam and Bowman,[41] and the data are presented in the format of that formulation. Probe power is monitored for approximately 30 s; the data are extrapolated to the ordinate intercept, which represents probe power $\Gamma$ at the steady state condition. With increasing perfusion, the steady state probe power increases, owing to the increase in effective conductivity.

Figure 6b demonstrates that, with sufficiently short measurement periods, it is possible to extrapolate the characteristic line to the steady state power density and thus to obtain, accurately, the effective thermal conductivity even with excess heat transfer caused by the proximity of large blood vessels. Based on these results, it was speculated that probe–vessel spacing and vessel size may be estimated from the time dependence and the magnitude of the deviation of the data from the characteristic, diffusion-controlled, power-vs.-time curve. By substituting the time that the deviation from the characteristic diffusion-controlled curve occurs into the time-dependent medium solution $V_m(r, t)$, the probe center to vessel (surface) distance, $r$, may be determined.[41–43] At any subsequent time the magnitude of the deviation is a measure of the heat-carrying capacity of the "thermally significant" vessel and thus a measure of its size. Although the methodology has not been

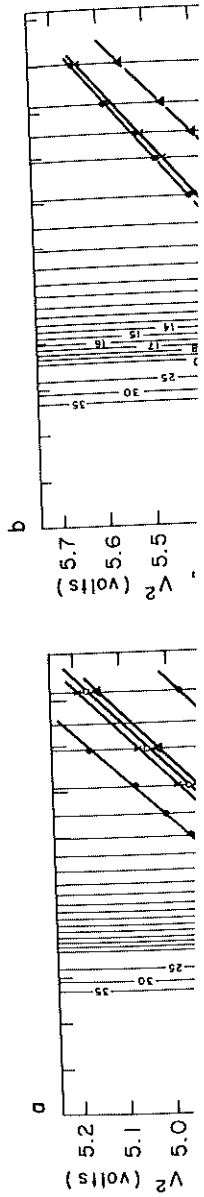

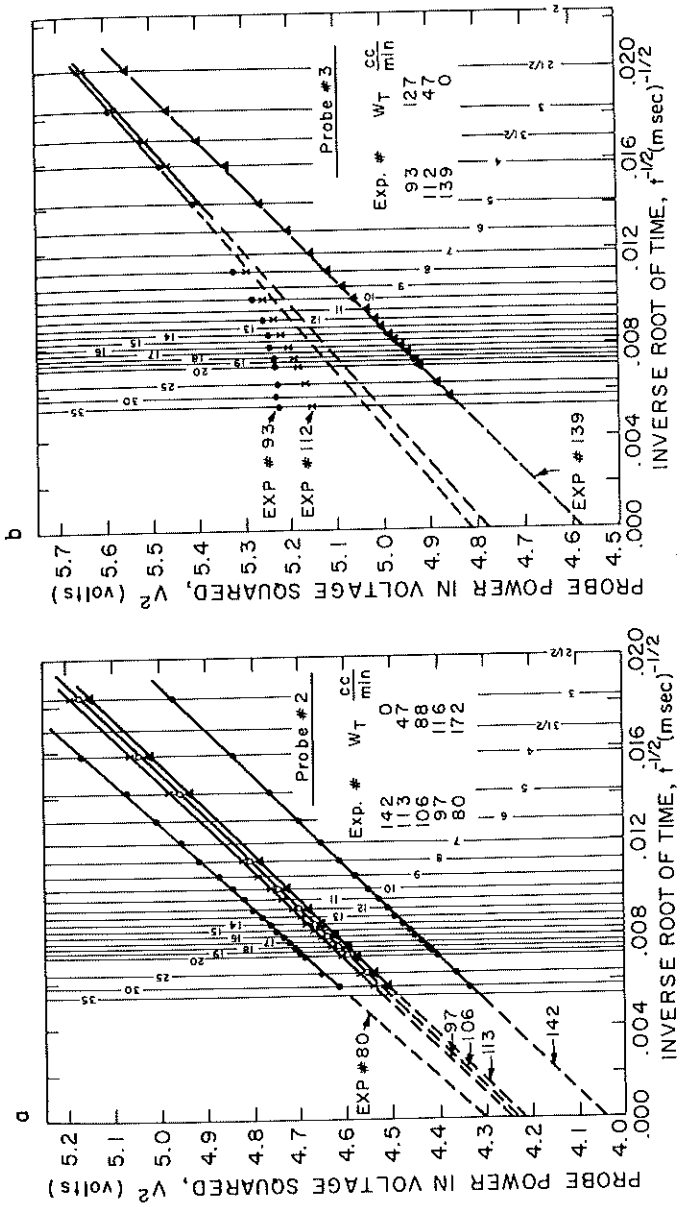


*FIGURE 6*
(a) Plot of probe transient power dissipation measured in the gracilis muscle as a function of total flow of the hind limb. (b) Same plot as in (a), when a "thermally significant" vessel is present in the region of thermal influence of the probe. (Reproduced from Ref. 28, with permission.)

developed at this time, Bowman[12] showed the validity of the rationale in model experiments.

### 7.2. Complete Solution of the Governing Equations for the Temperature Field

A complete solution to Eqs. (12)–(20), involving higher-order approximations for $V_p$ and $V_m$ in terms of $f(t)$, has recently been obtained by Valvano and Bowman.[17] The second-order system of partial differential equations can be converted into a second-order system of ordinary differential equations by introducing the unilateral Laplace transform. The key to finding the closed form, inverse Laplace transform is to express the Laplace domain solution as a Frobenius series and then perform a term-by-term inverse transform. The final closed form approximation of the two-region temperature field is given by

$$V_p(r, t) = \frac{a^2}{k_p}[\Gamma + \beta f(t)]\left[\frac{k_p}{3k_m(1+\sqrt{z})} + \frac{1}{6}\left(1 - \frac{r^2}{a^2}\right)\right] - \frac{\Gamma a^3 f(t)}{3k_m(\alpha_m \pi)^{1/2}(1-z)} \tag{35}$$

$$V_m(r, t) = \frac{\Gamma a^3}{3k_m r(1+\sqrt{z})}\left\{\exp\left[\sqrt{z}\left(1 - \frac{r}{a}\right)\right] + \frac{(a-r)f(t)}{(\alpha_m \pi)^{1/2}}\right\} - \frac{\Gamma a^4 f(t)}{3k_m r(\alpha_m \pi)^{1/2}(1-z)} + \frac{\beta a^3 f(t)}{3k_m r(1-\sqrt{z})} \tag{36}$$

where $z = \rho_b c_b w_b a^2 / k_m$. Note that the internal heat generation within the probe, $\Gamma + \beta f(t)$, can be separated into steady state and transient parts, where $\Gamma$ is the steady state volume average power and $\beta f(t)$ is the transient volume average power, both in W/ml. One further assumes that $f(t)$ tends to zero for large time. For this condition, the fact that the volume average transient temperature terms must add to zero can be used to derive an explicit expression for $f(t)$ in the presence of perfusion:

$$f(t) = \frac{\exp[-(\rho_b c_b w_b \alpha_m / k_m)t]}{\sqrt{t}} - \left(\frac{\rho_b c_b w_b \alpha_m \pi}{k_m}\right)^{1/2} \operatorname{erfc}\left(\frac{\rho_b c_b w_b \alpha_m t}{k_m}\right)^{1/2} \tag{37}$$

## 8. SIGNIFICANCE OF EXPANDED $f(t)$

In the absence of flow, Eq. (37) reveals that the transient power response does indeed follow $t^{-1/2}$. The $t^{-1/2}$ assumption originated with the lumped analysis of Chato,[40] where the transient heat flux for a fixed probe surface temperature was shown to follow $t^{-1/2}$. The transient nonperfused coupled

*FIGURE 7*
Measurement errors in $\Gamma$, $k_{eff}$, an
are calculated as a functio
perfusion when a $t^{-1/2}$ tra
power response is assumed. Wh
true power transient, $\Gamma + \beta f(t)$ is
to $\Gamma + \beta t^{-1/2}$, errors result in b
and $\beta$. The magnitude of these
increases with perfusion rate.

probe–tissue analysis of
dependence for the pro
measured power in the
This was due to the fa
10 ml/100 g min.

As can be seen fror
and $t^{-1/2}$ increases wit
transient response follo
regression of transient
intercept $\Gamma$ and the slo
in Fig. 7 as a function

In principle, the s
a third measure of per
due to high perfusion
vessel are similar. In a
the shape of the trans
discriminate between
response as a third m
transfer capacity of a

## 9. APPLICATION O
## DERIVE PERFU

Balasubramanian
the volume average t
can be used to calcul
values of applied and

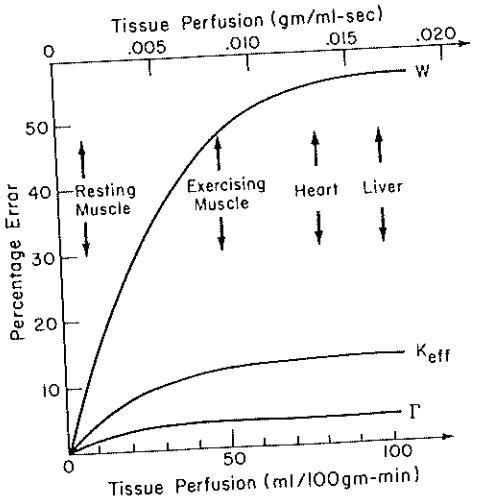


*FIGURE 7*
Measurement errors in $\Gamma$, $k_{eff}$, and $w_b$, are calculated as a function of perfusion when a $t^{-1/2}$ transient power response is assumed. When the true power transient, $\Gamma + \beta f(t)$ is fitted to $\Gamma + \beta t^{-1/2}$, errors result in both $\Gamma$ and $\beta$. The magnitude of these errors increases with perfusion rate.

probe–tissue analysis of Balasubramaniam and Bowman[41–43] used a $t^{-1/2}$ dependence for the probe volumetric heat generation. The experimentally measured power in the presence of perfusion also appeared to follow $t^{-1/2}$.[28] This was due to the fact that normal gracilis muscle perfusion is only 5–10 ml/100 g min.

As can be seen from Eq. (37), the difference between the expanded $f(t)$ and $t^{-1/2}$ increases with time and perfusion rate. If one assumes that the transient response follows $t^{-1/2}$ in the presence of perfusion, the least-squares regression of transient power (from 4 to 10 s) will result in errors in both the intercept $\Gamma$ and the slope $\beta$. The resulting errors in $\Gamma$, $k_{eff}$, and $w_b$ are plotted in Fig. 7 as a function of perfusion rate.

In principle, the shape of the transient response itself could be used as a third measure of perfusion. However, the shape of the transient response due to high perfusion and that due to proximity of a thermally significant vessel are similar. In addition, a time-varying tissue temperature also affects the shape of the transient power response. It thus would be necessary to discriminate between these effects in order to use the shape of the transient response as a third measure of flow, or to quantify the location and heat transfer capacity of a nearby vessel.

## 9. APPLICATION OF THE TRANSIENT THERMAL MODEL TO DERIVE PERFUSION

Balasubramanian and Bowman[28] integrated $V_p(r, t)$ from 0 to $a$, to find the volume average temperature increment, $\Delta T_p$. This steady state solution can be used to calculate the effective thermal conductivity from measured values of applied and imposed temperature increment. Rearranging Eq. (30),

$$k_{eff} = \frac{1}{(3\Delta T_p/\Gamma a^2) - 0.2/k_p} \tag{38}$$

In the absence of flow, $k_{\text{eff}}$ equals $k_m$. The bead is supplied with electrical power at a rate, $(\Gamma + \beta t^{-1/2})$, sufficient to maintain the bead at a constant temperature increment above the tissue baseline temperature $T_0$. The transient power response plotted vs. $t^{-1/2}$ is a straight line for diffusion-controlled processes. A linear regression is performed to find $\Gamma$, and thus to calculate $k_{\text{eff}}$. This is the same method to obtain perfusion as was previously described.

Consideration of the transient solution for the temperature field in tissue, Eqs. (35) and (36), leads to an alternative method to extract the perfusion parameter. As mentioned, the volume-averaged temperature within the bead is held constant by the instrument. Thus, the volume-averaged temperature within the bead due to the transient terms from $\Gamma$ are equal and opposite of those due to $\beta f(t)$, and their sum must add to zero at all times.[41,44] Thus, it can be shown that[45,46]

$$\alpha_{\text{eff}} = \left[\frac{a}{(\sqrt{\pi}\beta/\Gamma)(1 + 0.2k_m/k_p)}\right]^2 \tag{39}$$

In the absence of flow, $\alpha_{\text{eff}}$ equals $\alpha_m$ and $\beta/\Gamma$ can be calculated by least-squares regression of the measured transient power, equal to $\Gamma + \beta t^{-1/2}$.

Thus the perfusion term, $w_b$, can be isolated from both the steady state[28] and transient solutions.[17,46] The second measure of perfusion is unique to the transient solution, and we denote it $w_{b2}$:

$$w_b = \left(\frac{k_{\text{eff}}}{k_m} - 1\right)^2 \frac{k_m}{\rho_b c_b a^2} \tag{40}$$

$$w_{b2} = \frac{(\sqrt{\alpha_{\text{eff}}} - \sqrt{\alpha_m})^2}{\alpha_m \rho_b c_b a^2}\left(1 + 0.2\frac{k_m}{k_p}\right)^2 k_m \tag{41}$$

## 10. PERFUSION MEASUREMENT PROTOCOL

Our present protocol for quantifying perfusion in small volumes of tissue using the thermistor bead apparatus, which we call the thermal diffusion probe, and taking advantage of the solution to the complete governing equations, is as follows:

1. Apply the volume-averaged temperature increment, $\Delta T_p$;
2. Record the transient voltage required to maintain the volume-averaged $\Delta T_p$;
3. Perform a least-squares regression using $\Gamma + \beta t^{-1/2}$ to find an approximate value of $\Gamma$;
4. Use Eq. (38) to calculate an approximate $k_{\text{eff}}$;
5. Use Eq. (40) to calculate an approximate $w_b$;
6. Perform a least-squares regression using $\Gamma + \beta f(t)$ to find $\Gamma$ and $\beta$, where $f(t)$ is evaluated using Eq. (37) and the approximate value of $w_b$ found in step 5;
7. Iterate steps 4, 5,
   usually sufficient
8. Use Eqs. (38) and
9. Use Eqs. (40) and

Sometimes the noise
process does not lead to
the errors of the least-squ
may first lead to a better
due to error multiplicatic
which yields the best fit

## 11. THE THERMAL D

The thermal diffusi
which has the capabilit
thermal conductivity, th
transient measurement i
important in a number
system utilizes a therm
operated in either conti
perature, thermal condu
tioned, in the transient
characterize thermally
distance from the probe

The characteristics
The bead is interfaced v
based data acquisition
developed over the pa
providing accurate real
ties, and perfusion in s
following standard co
real-time clock, plottin
instrument incorporate
routines, and mass stor
two special modules: a
A controller module all
(2) application and m
simultaneous operation
of two modes (transient
tion of effective therm

In the transient m
a measure of the effecti
section, the intrinsic t

* Rollins Associates, Concor

7. Iterate steps 4, 5, 6; our experience indicates that three iterations are usually sufficient to converge within 1% of the stable value of $k_{eff}$;
8. Use Eqs. (38) and (39) to calculate $k_{eff}$ and $\alpha_{eff}$;
9. Use Eqs. (40) and (41) to calculate $w_b$.

Sometimes the noise in the original $V^2$ vs. $t$ data is such that the iteration process does not lead to convergence of $k_{eff}$, $w_b$, or $\sigma$, where $\sigma$ is the sum of the errors of the least-squares regression. In these situations multiple iterations may first lead to a better or improved fit and then to increasingly worse fits due to error multiplication. Best results are usually obtained for that iteration which yields the best fit as defined by smallest $\sigma$.

## 11. THE THERMAL DIFFUSION PROBE

The thermal diffusion probe* (TDP) is a versatile, portable instrument which has the capability of quantifying temperature, intrinsic or effective thermal conductivity, thermal diffusivity, and perfusion from a single 10–20 s transient measurement in small volumes of tissue. These four parameters are important in a number of clinical applications. The microprocessor-based system utilizes a thermistor tipped needle or catheter probe, and can be operated in either continuous or repetitive transient modes to measure temperature, thermal conductivity, thermal diffusivity, and/or perfusion. As mentioned, in the transient mode of operation the technique is also able to characterize thermally significant vessels in the tissue according to their distance from the probe and their heat-carrying capacity.[12]

The characteristics of the heated thermistor bead were described earlier. The bead is interfaced with the TDP instrument, a modular, microprocessor-based data acquisition–controller system, Fig. 8. This system has been developed over the past decade to facilitate bioheat transfer research by providing accurate real-time measurements of temperature, thermal properties, and perfusion in small volumes of tissue. The instrument contains the following standard computer modules: Z80 CPU, 16K ROM, 48K RAM, real-time clock, plotting CRT, and a $5\frac{1}{4}$-in. mini floppy twin disk drive. The instrument incorporates flexible operator control, sophisticated plotting routines, and mass storage on the mini floppy disk. The system also includes two special modules: a 14-bit A/D converter and thermal probe controllers. A controller module allows (1) measurement of base-line tissue temperature; (2) application and measurement of power supplied to the thermistor; (3) simultaneous operation of four thermistor probes; and (4) operation in either of two modes (transient and continuous), both of which allow the determination of effective thermal conductivity.

In the transient mode, the probe power, extrapolated to infinite time, is a measure of the effective thermal conductivity. As discussed in the previous section, the intrinsic thermal conductivity of the tissue must be provided,

* Rollins Associates, Concord Rd., Lincoln, Massachusetts.

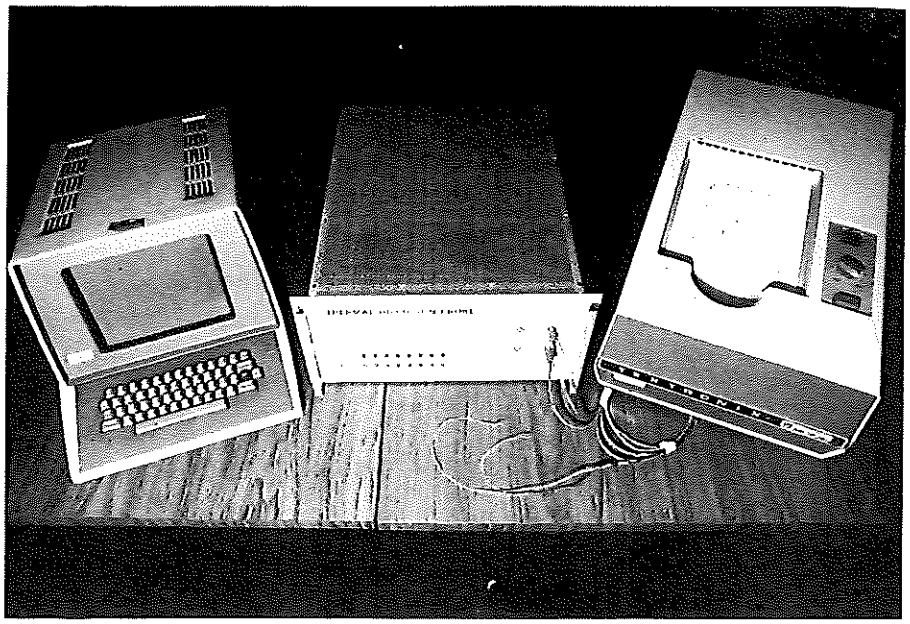

*FIGURE 8*
The prototype microprocessor–TDP system.

by a separate keyboard entry, by the two-bead method, or by a determination involving blood occlusion at some point in the measurement protocol. In this mode, flow can be measured approximately once a minute, and the effective volume of tissue perturbed and monitored by the probe can be varied over a wide range.

In the continuous mode, the system monitors both the heated probe power requirement and the tissue temperature (using a second thermistor located at a point outside the region of thermal influence of the heated probe). In this mode, flow is monitored continuously

When operating in the temperature monitoring mode, the temperature plotting routine can be repeatedly interrupted at will to update the effective thermal conductivity. This is an excellent measure of "unexpected" changes in tissue heat transfer properties, mainly perfusion.

*Example.* For understanding better the measurement and data reduction protocols for quantification of perfusion from effective thermal conductivity, four experiments from a single isolated perfused rat liver preparation will be cited. Total blood flow was measured by venous collection, and the local level of perfusion was calculated by proportioning the total flow in accordance with the distribution of entrapped radioactive microspheres.

Probe No. B31x was introduced into the left lobe of the 5.770-g liver removed from a 380-g rat in accordance with an established protocol.[17,47] Liver volume was measured as 5.00 ml giving a density of 1.154 g/ml. The probe constants, $k_p = 1.021$ mW/cm K and radius $a = 0.0888$ cm were determined from calibration data.

The total blood flo
after each experiment
13.30 ml/min. The loca
the probe was determi
of the known total flo
radioactive microsphe
experiment 109 becau
in this experiment was
Experiment 127 was a

Before each meas
when stable, a tempera
in the thermistor bead
maintain the imposed

| Variables | |
|---|---|
| $T_s$ (°C) | |
| $R_H$ (Ω) | |
| $\Delta T$ (°C) | |
| $F$ (ml/min) | |
| $\bar{w}$ (g/ml s) ($\times 10^{-3}$) | |
| $w_T$ (g/ml s) ($\times 10^{-3}$) | |
| Time (s) | |
| 4.0 | |
| 4.5 | |
| 5.0 | |
| 5.5 | |
| 6.0 | |
| 6.5 | |
| 7.0 | |
| 7.5 | |
| 8.0 | |
| 8.5 | |
| 9.0 | |
| 9.5 | |
| 10.0 | |
| 10.5 | |
| 11.0 | |
| 11.5 | |
| 12.0 | |

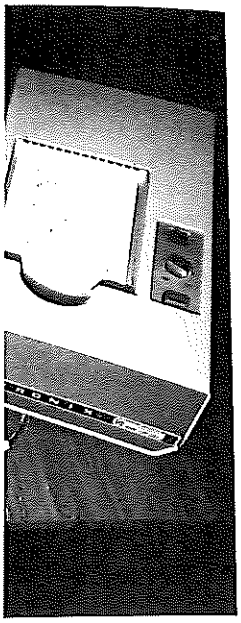

or by a determination
ment protocol. In this
ute, and the effective
can be varied over a

oth the heated probe
; a second thermistor
e of the heated probe).

ode, the temperature
o update the effective
'unexpected" changes

nt and data reduction
thermal conductivity,
er preparation will be
lection, and the local
otal flow in accordance
heres.
ie of the 5.770-g liver
blished protocol.[17,47]
ity of 1.154 g/ml. The
0.0888 cm were deter-



The total blood flow, $F$, was measured by venous collection before and after each experimental transient run. Total flow was varied from zero to 13.30 ml/min. The local perfusion ($w_T$) in the tissue immediately surrounding the probe was determined in experiments 106 and 119 from apportionment of the known total flow in accordance with the distribution of entrapped radioactive microspheres (Table 2). This measurement was not possible in experiment 109 because of a limited number of radiolabels. Therefore flow, in this experiment was apportioned as was done for experiments 106 and 119. Experiment 127 was a no-flow control.

Before each measurement, the tissue temperature was monitored, and when stable, a temperature increment $\Delta T_p$ of approximately 4°C was imposed in the thermistor bead. The squares of the voltages required to establish and maintain the imposed $\Delta T_p$ are tabulated in Table 2 as a function of time for

*TABLE 2*

| | Experiment number | | | |
|---|---|---|---|---|
| Variables | 127 | 106 | 109 | 119 |
| $T_s$ (°C) | 33.995 | 33.995 | 35.037 | 35.694 |
| $R_H$ ($\Omega$) | 645.1 | 625.2 | 605.5 | 585.6 |
| $\Delta T$ (°C) | 4.066 | 3.938 | 3.796 | 4.087 |
| $F$ (ml/min) | 0.00 | 3.56 | 7.58 | 13.30 |
| $\bar{w}$ (g/ml s) ($\times 10^{-3}$) | 0.00 | 11.9 | 25.3 | 44.3 |
| $w_T$ (g/ml s) ($\times 10^{-3}$) | 0.00 | 14.0 | 29.7 | 52.1 |
| Time (s) | Bead voltage squared ($V^2$) | | | |
| 4.0 | 9.509 | 9.134 | 8.631 | 9.136 |
| 4.5 | 9.401 | 9.406 | 8.544 | 9.059 |
| 5.0 | 9.308 | 8.964 | 8.466 | 8.995 |
| 5.5 | 9.226 | 8.897 | 8.406 | 8.934 |
| 6.0 | 9.158 | 8.841 | 8.351 | 8.888 |
| 6.5 | 9.097 | 8.739 | 8.302 | 8.845 |
| 7.0 | 9.037 | 8.724 | 8.265 | 8.805 |
| 7.5 | 8.990 | 8.704 | 8.229 | 8.772 |
| 8.0 | 8.942 | 8.667 | 8.201 | 8.744 |
| 8.5 | 8.895 | 8.636 | 8.166 | 8.719 |
| 9.0 | 8.857 | 8.604 | 8.140 | 8.694 |
| 9.5 | 8.821 | 8.759 | 8.116 | 8.670 |
| 10.0 | 8.787 | 8.551 | 8.097 | 8.658 |
| 10.5 | 8.753 | 8.528 | 8.073 | 8.636 |
| 11.0 | 8.722 | 8.513 | 8.055 | 8.618 |
| 11.5 | 8.690 | 8.489 | 8.036 | 8.602 |
| 12.0 | 8.667 | 8.469 | 8.019 | 8.592 |

each of the four experimental runs with total flows of 0, 3.56, 7.58, and 13.30 ml/min. The average and true local tissue perfusions are noted as $\bar{w}$ and $w_T$, respectively.

As discussed in step 3, a least-squares regression $V^2 = \Gamma + \beta t^{-1/2}$ is first performed using the $V^2(t)$ data of Table 2 to find approximate values of $\Gamma$; $k_{\text{eff}}$ is calculated from Eq. (38), and $w_b$ is calculated, using Eq. (40). In step 6 a least-squares regression $V^2 = \Gamma + \beta f(t)$ is then performed using the same data to reevaluate $\Gamma$ and $\beta$, where $f(t)$ is evaluated using Eq. (37) and the approximate value of $w_b$ found in the first regression.

As seen in Table 3, successive iterations generally lead to convergence of $k_{\text{eff}}$ and thus of $w_b$. As noted above, noise in the original $V^2$ vs. $t$ data will sometimes hinder convergence of $\sigma$, the sum of the errors of the least-squared regression. In these situations, as is the case in this example, multiple iterations may first lead to a better fit and then to increasingly worse fits due to error

*TABLE 3*

| Iteration | $\sigma$ | $s/I$ ($s^{1/2}$) | SP ($K/W$) ×10 | $k_{\text{eff}}$ (W/cm K) ×$10^3$ | $\rho_b w_b$ (g/ml s) ×$10^3$ | $z = \frac{\rho_b c_b w_b a^2}{k_m}$ ($s^{1/2}$) |
|---|---|---|---|---|---|---|
| | | | | | | 0.00000 |
| 106-0 | 0.00308 | 0.4161 | 325.8 | 5.966 | 3.132 | 0.00354 |
| -1 | 0.00248 | 0.4114 | 314.1 | 6.465 | 8.812 | 0.00996 |
| -2 | 0.00178 | 0.4227 | 308.6 | 6.735 | 13.087* | 0.01479 |
| -3 | 0.00186 | 0.4337 | 306.1 | 6.862 | 15.396* | 0.01740 |
| -4 | 0.00212 | 0.4402 | 305.1 | 6.917 | 16.457 | 0.01860 |
| -5 | 0.00228 | 0.4432 | 304.6 | 6.941 | 16.920 | 0.01912 |
| -6 | 0.00235 | 0.4445 | 304.5 | 6.950 | 17.107 | 0.01933 |
| -7 | 0.00238 | 0.4451 | 304.4 | 6.955 | 17.197 | 0.01943 |
| | | | | | | 0.00000 |
| 109-0 | 0.00519 | 0.3992 | 319.9 | 6.208 | 5.536 | 0.00626 |
| -1 | 0.00412 | 0.3994 | 306.2 | 6.858 | 15.320 | 0.01731 |
| -2 | 0.00262 | 0.4233 | 300.4 | 7.178 | 21.929 | 0.02478 |
| -3 | 0.00230 | 0.4424 | 298.1 | 7.310 | 24.991* | 0.02824 |
| -4 | 0.00245 | 0.4519 | 297.3 | 7.360 | 26.208* | 0.02962 |
| -5 | 0.00255 | 0.4557 | 297.0 | 7.378 | 26.659 | 0.03013 |
| -6 | 0.00259 | 0.4572 | 296.9 | 7.385 | 26.828 | 0.03032 |
| -7 | 0.00261 | 0.4577 | 296.8 | 7.387 | 26.890 | 0.03039 |
| | | | | | | 0.00000 |
| 119-0 | 0.00551 | 0.3300 | 305.5 | 6.898 | 16.073 | 0.01810 |
| -1 | 0.00281 | 0.3554 | 289.7 | 7.851 | 39.700 | 0.04486 |
| -2 | 0.00349 | 0.4204 | 285.0 | 8.183 | 50.375* | 0.05692 |
| -3 | 0.00529 | 0.4543 | 283.8 | 8.274 | 53.531* | 0.06049 |
| -4 | 0.00585 | 0.4648 | 283.5 | 8.298 | 54.364 | 0.06143 |
| -5 | 0.00600 | 0.4677 | 283.5 | 8.304 | 54.575 | 0.06167 |
| -6 | 0.00604 | 0.4684 | 283.4 | 8.305 | 54.608 | 0.06171 |
| -7 | 0.00605 | 0.4685 | 283.4 | 8.306 | 54.651 | 0.06176 |
| 127-0 | 0.00616 | 0.5308 | 348.7 | 5.229 | 0.000 | 0.00000 |

NOTE: Asterisk indicates iteration of best fit.

multiplication. In these
($n$) which yields the bes
which uses the data de
accurate to within ±10
ably accurate (±1.0%)

## 12. EXPERIMENTAL

### 12.1. Accuracy of The

The values of $k_p$
calibration, using two l
and glycerin) as don
accuracy of measurem
and 10, respectively.
50%/50%, and 75%/2
ments within 1%–2%

The TDP is sensit
until recently how acc
has been to find a tissu
and independently. W
isolated canine gracili
preparations. We have
perfused rat liver prep
to quantify perfusion

Figure 11 is a blc
used to establish the
reservoir, through a
back to a reservoir. Tl
to oxygenate the perf
and open loop flow
resistance pinch valv

*FIGURE 9*
Thermal conductivity as
Diffusion Probe is plotte
conductivity. The five
glycerin, and three water
thermal conductivity of
determined from its ma
measurement error is 1.

multiplication. In these cases best results are usually obtained for iteration $(n)$ which yields the best fit as defined by the smallest $\sigma$, or by iteration $(n+1)$ which uses the data derived from iteration $(n)$. The technique is generally accurate to within ±10%; however, the method is dependent upon a reasonably accurate (±1.0%) value of intrinsic thermal conductivity $k_m$.

## 12. EXPERIMENTAL VERIFICATION

### 12.1. Accuracy of Thermal Property and Perfusion Measurements

The values of $k_p$ and $a$ for the perfusion probe are determined by calibration, using two liquids with known thermal properties (1.5% agar–water and glycerin) as done for the original thermal conductivity probe. The accuracy of measurements of $k_m$ and $\alpha_m$ with the TDP is shown in Figs. 9 and 10, respectively. Using three glycerin/water mixtures (25%/75%, 50%/50%, and 75%/25%) it was verified that the TDP is capable of measurements within 1%–2% of the true values.

The TDP is sensitive to changes in perfusion, but it has not been resolved until recently how accurately it can quantify perfusion. The biggest problem has been to find a tissue model in which perfusion can be assessed accurately and independently. We have previously used isolated canine hind limbs,[28] isolated canine gracilis muscle,[48] and isolated canine myocardial pedicle[49] preparations. We have recently begun to use the isolated, thermally regulated, perfused rat liver preparation[47] to evaluate the ability of the TDP instrument to quantify perfusion.[17]

Figure 11 is a block diagram of the perfusion apparatus.[17,47] A pump is used to establish the circulation of Krebs–Ringer buffer perfusate from a reservoir, through a Millipore paper filter, heat exchanger, oxygenator, and back to a reservoir. This closed loop cycle (method of Brunengraber[50]) serves to oxygenate the perfusate and establish a constant pressure head. Both closed and open loop flow to the liver preparation is controlled via a variable resistance pinch valve. Flow enters the liver through the cannulated portal

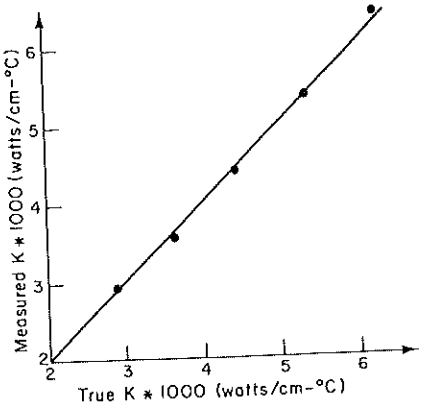


*FIGURE 9*
Thermal conductivity as measured by the Thermal Diffusion Probe is plotted versus the true thermal conductivity. The five liquid media are water, glycerin, and three water/glycerin mixes. The true thermal conductivity of a water/glycerin mix is determined from its mass fraction. The average measurement error is 1.5%.

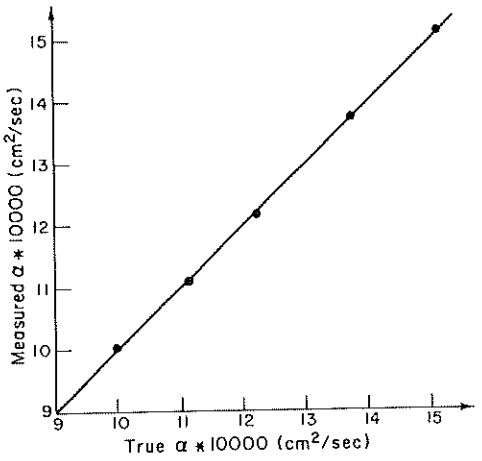


*FIGURE 10*
Thermal diffusivity as measured by the thermal diffusion probe is plotted versus the true thermal diffusivity. The five liquid media are water, glycerin, and three water/glycerin mixes. The true thermal diffusivity of a water/glycerin mix is determined from its mass fraction. The average measurement error is 0.9%.

vein and leaves via the cannulated inferior vena cava. The total flow is collected and measured with a mass balance and a stop watch. The open loop perfusion system was chosen to avoid contaminating the entire apparatus when radiolabeled microspheres are injected, and to maintain liver perfusion with fresh buffer.

The establishment and maintenance of temperature stability is critical for the accurate thermal measurement of tissue perfusion. One hundred percent humidity is maintained within the enclosed box to reduce cooling due to evaporation at the surface of the liver. Both the 100% humidity and a plastic wrap reduce convective and evaporative cooling of the liver and therefore minimize temperature gradients within the liver. Continuous attention must be given to the establishment and maintenance of thermal equilibrium within the rat liver, in order to allow the accurate and reproducible measurement of tissue perfusion. Temperature stability better than

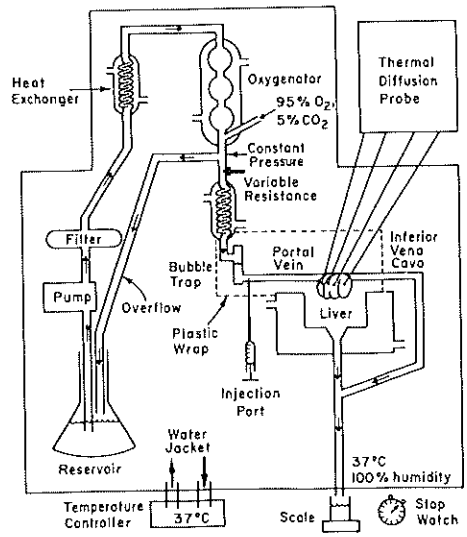


*FIGURE 11*
Block diagram of the isolated rat liver preparation used to evaluate the Thermal Diffusion Probe.

*FIGURE*
Thermisto

0.003°C/min and flow s
within the preparation. I
tissue (Fig. 12), and $T$, $k_e$
run, using the TDP.

Radioactive microsp
of perfusion within the
tion of perfusion was

*FIGURE 13*
Tissue perfusion, as measur
tive microsphere technique,
various sections of the rat live
variations are much larger t
within a single lobe.

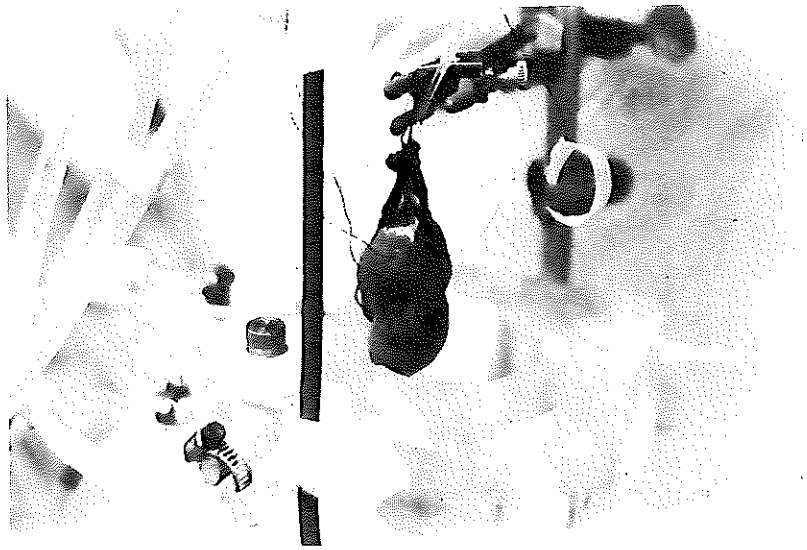

*FIGURE 12*
Thermistor probes in place in the rat liver preparation.

0.003°C/min and flow stability of 0.01 ml/min per min can be maintained within the preparation. Multiple thermistor probes are inserted in the hepatic tissue (Fig. 12), and $T$, $k_{\text{eff}}$, $\alpha_{\text{eff}}$, and $w_b$ are measured for each thermal transient run, using the TDP.

Radioactive microspheres are used to determine the spatial distribution of perfusion within the isolated rat liver.[47,51] In general the spatial distribution of perfusion was found to vary somewhat with time, although total

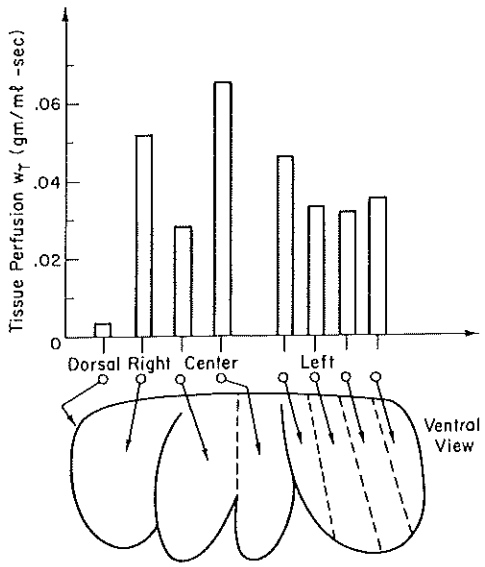


*FIGURE 13*
Tissue perfusion, as measured by radioactive microsphere technique, is plotted for various sections of the rat liver. Lobe to lobe variations are much larger than variations within a single lobe.

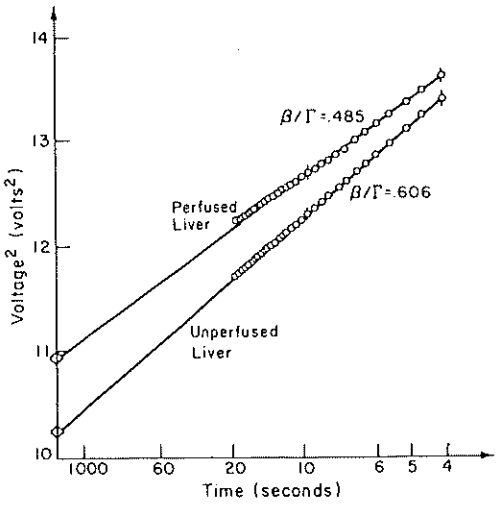


*FIGURE 14*
$V_s^2$ vs. $t^{-1/2}$ transient responses for experiments in the isolated rat liver preparation. The same probe and $\Delta T_i$ were employed at the same site for both runs. See text for details.

perfusion was maintained constant. At the termination of the rat liver perfusion measurements, flow is interrupted and the intrinsic thermal properties are measured. The liver is sectioned (about 1 ml surrounding the probe) and the radioactivity of each piece is measured. The relative radioactivity of any liver segment is equal to the relative flow to that segment. Thus, the true perfusion distribution can be calculated. Repeated counts reveal a reproducibility of 1.8% in the measured radioactivity for each liver section. When the three labels ($^{113}$Sn, $^{141}$Ce, and $^{57}$Co) were injected two minutes apart, they gave consistent measurements to within 2%. The shunt fraction was found to be 0.6%. Lobe-to-lobe variations in perfusion were much larger than variations within a single lobe (Fig. 13).

Figure 14 contains two transient power responses plotted on the same graph measured with the same probe using the same temperature increment.

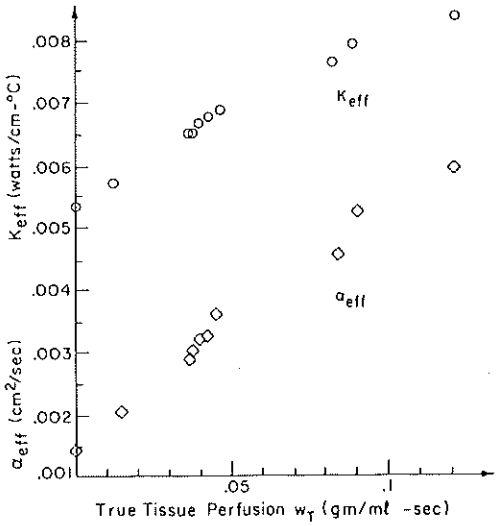


*FIGURE 15*
"Effective" thermal properties are here graphed vs. tissue perfusion in the isolated rat liver. $k_{eff}$ and $\alpha_{eff}$ are measured using the Thermal Diffusion Probe. $w_T$ is calculated from the total collected flow, corrected by radioactive microsphere results.

*FIGURE 16*
Thermal perfusion as measure
Thermal Diffusion Probe is pl
the true tissue perfusion as n
by the total collected flow c
by radioactive microsphere
Equation (40) was used to c
perfusion from measured $k_{eff}$.

The top curve was ob
(120 ml/100 g min); the
The presence of flow i
increased $k_{eff}$ according
in an increased $\alpha_{eff}$ ac
curvature of the transie
fitted to a $\Gamma + \beta t^{-1/2}$ axi

Figure 15 displays
$k_{eff}$ and $\alpha_{eff}$ are quite s
changes in perfusion ra
measurements at the sar
$k_{eff}$ better than 0.6% an
results in a reproducibi

*FIGURE 17*
Tissue perfusion as measured
mal Diffusion Probe is plotte
tissue perfusion as measured
collected flow corrected by
microspheres. Equation (41)
calculate perfusion from mea

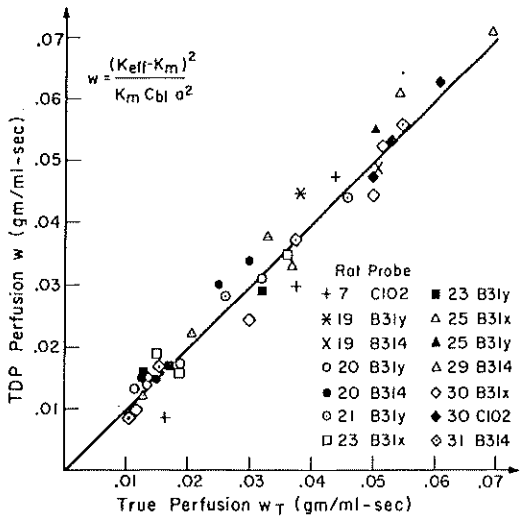


*FIGURE 16*
Thermal perfusion as measured by the Thermal Diffusion Probe is plotted vs. the true tissue perfusion as measured by the total collected flow corrected by radioactive microsphere results. Equation (40) was used to calculate perfusion from measured $k_{eff}$.

The top curve was obtained when the liver was perfused at 0.02 g/ml s (120 ml/100 g min); the bottom curve resulted when flow was interrupted. The presence of flow increases the steady state intercept, $\Gamma$, resulting in an increased $k_{eff}$ according to Eq. (38). Flow decreases the $\beta/\Gamma$ ratio, resulting in an increased $\alpha_{eff}$ according to Eq. (39), and produces a slight upward curvature of the transient response, because the true $\Gamma + \beta f(t)$ transient was fitted to a $\Gamma + \beta t^{-1/2}$ axis.

Figure 15 displays typical experimental results, which shows that both $k_{eff}$ and $\alpha_{eff}$ are quite sensitive to perfusion. While $\alpha_{eff}$ is more sensitive to changes in perfusion rate than $k_{eff}$, it is somewhat less reproducible. Multiple measurements at the same flow rate reveal an experimental reproducibility in $k_{eff}$ better than 0.6% and in $\alpha_{eff}$ better than 2%. When Eq. (40) is used, this results in a reproducibility in calculated perfusion of about 5%. Meticulous

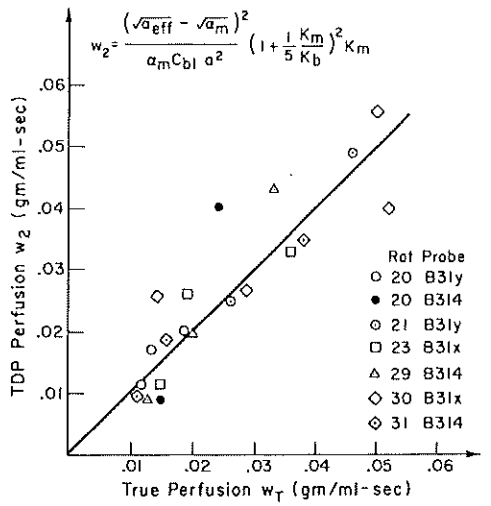


*FIGURE 17*
Tissue perfusion as measured by the Thermal Diffusion Probe is plotted vs. the true tissue perfusion as measured by the total collected flow corrected by radioactive microspheres. Equation (41) was used to calculate perfusion from measured $\alpha_{eff}$.

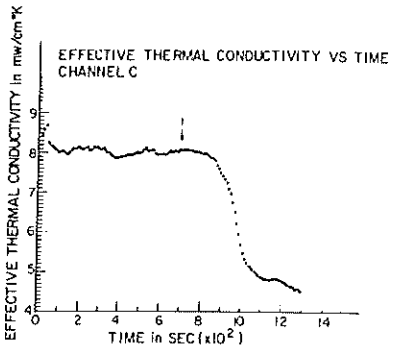


*FIGURE 18*
Typical display of local effective thermal conductivity measured in isolated canine gracilis muscle. This 1300-s record includes the effect of shut-off of respiratory airflow to the intubated animal at 700 s. The elevation of effective thermal conductivity above the intrinsic value obtained in the unperfused, expired animal at 1,300 s is a measure of the convection-augmented heat dissipation due to perfusion.

attention given to the establishment of tissue thermal equilibrium will guarantee reproducible measurements. Since the TDP instrument can easily discriminate 1% changes in $k_{eff}$, it will have a sensitivity to perfusion of better than 7%.

Collected results from several experiments are given in Figs. 16 and 17. Absolute values of TDP-derived local perfusion rates are plotted against the independently measured local perfusion rate for the same region of the same lobe. This rate is obtained by weighting the volumetrically measured total flow by the ratio of radiolabeled microsphere activity in the sample of tissue surrounding the TDP probe to total radiolabel activity of the liver. Good agreement is obtained for the $k_{eff}$ method (Fig. 16). An average measurement error of ±10.6% is obtained, with uniform scatter about the line of identity, for 14 different studies. Results with the $\alpha_{eff}$ method were somewhat less satisfactory (Fig. 17). The average perfusion measurement error was 24%, with a skew about the identity line. However, improved results are anticipated when probe stem heat leakage is accounted for and the probe design is improved.

### *12.2. Examples in Various Tissues*

Various features of data presentation of the TDP system, when operated in continuous mode, are shown in Figs. 18 and 19. The effect of perfusion on the value of $k_{eff}$ is shown in Fig. 18 for a canine gracilis muscle preparation. At 700 s the respirator for the intubated animal was shut off, and the

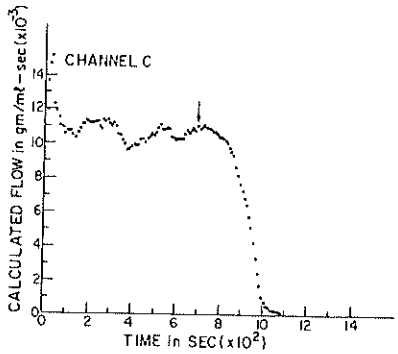


*FIGURE 19*
Typical display of local tissue perfusion derived from effective thermal conductivity measurements in an isolated canine gracilis muscle. This record reflects the temporal variations in local tissue perfusion before and after respirator shut-off at 700 s.

*FIGURE 20*
Real-time measurement of tis
line) and base-line tissue temp
using the Thermal Diffusion P
placed in a 7.25-g pedicle prep
the canine myocardium. Fro
coronary artery feeding the pe
With restoration of flow, reac
observed.

convective contribution
replotted as perfusion i
response to the respirat
gracilis muscle perfusion
approximately 4 min. Tl
skeletal muscle beds of t

The ability of the pr
the coupling between bl
21. The temperature of
relatively insensitive to sl
interruption of flow to t
subsequent reduction of t
dium and hind limb prep
was removed, and an inc
observed. The ability to r
this instrument, will be
ischemia, hyperthermia,
the nature and magnitud
amplitude of the temper
be different for various ti
tumor and normal tissue
have an important beari
(thermal and radiation t

*FIGURE 21*
Real-time measurement of tissu
line) and base-line tissue temper
using the Thermal Diffusion F
was placed in the hind limb of
was interrupted by applying a
approximately 170 to 260 s. W
flow, reactive hyperemia was ob

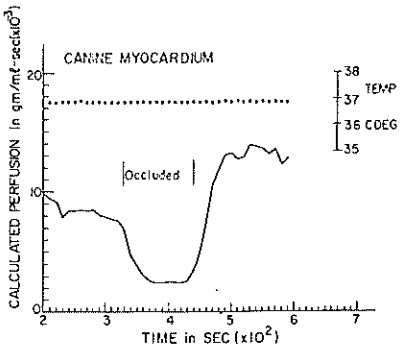


*FIGURE 20*
Real-time measurement of tissue perfusion (solid line) and base-line tissue temperature (dotted line) using the Thermal Diffusion Probe. The probe was placed in a 7.25-g pedicle preparation, isolated from the canine myocardium. From 330 to 430 s the coronary artery feeding the pedicle was occluded. With restoration of flow, reactive hyperemia was observed.

convective contribution to $k_{eff}$ declined over the next 10 min. These data are replotted as perfusion in Fig. 19. Note that perfusion declines to zero in response to the respiratory arrest. In addition, a phasic oscillation in the gracilis muscle perfusion is noted prior to respiratory arrest, with a period of approximately 4 min. This phasic behavior has also been observed in the skeletal muscle beds of the dog and the rat, and is believed to be typical.

The ability of the probe to follow the dynamics of local blood flow and the coupling between blood and tissue temperature is shown in Figs. 20 and 21. The temperature of canine myocardium (within the thoracic cavity) is relatively insensitive to short interruptions of blood flow (Fig. 20). In contrast, interruption of flow to the hind limb alters the limb heat balance with a subsequent reduction of temperature, as shown in Fig. 21. In both the myocardium and hind limb preparations flow was quickly restored when the clamp was removed, and an increase in flow, suggestive of reactive hyperemia, was observed. The ability to monitor continuously local perfusion, obtained with this instrument, will be of value in more fully understanding the effects of ischemia, hyperthermia, etc. on the local blood circulation. In hyperthermia the nature and magnitude of the change in tissue perfusion is related to the amplitude of the temperature elevation and its duration, and is believed to be different for various tissues. For example, the effects of hyperthermia on tumor and normal tissue blood perfusion, and therefore on their oxygenation, have an important bearing on the sequence in which different treatments (thermal and radiation therapy) should be used for maximal therapeutic

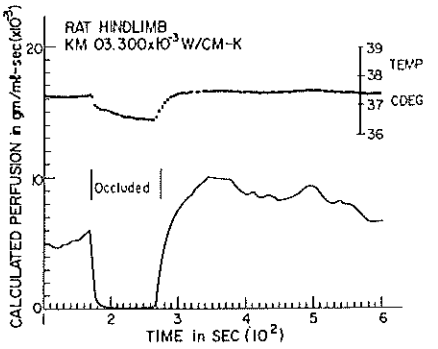


*FIGURE 21*
Real-time measurement of tissue perfusion (solid line) and base-line tissue temperature (dotted line) using the Thermal Diffusion Probe. The probe was placed in the hind limb of a 300-g rat. Flow was interrupted by applying a tourniquet from approximately 170 to 260 s. With restoration of flow, reactive hyperemia was observed.

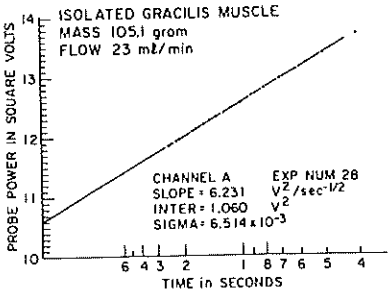


*FIGURE 22*
Typical plot of probe power vs. $t^{-1/2}$ for a diffusion-controlled process.

efficacy since the level of oxygenation influences the radiosensitivity of the cells. Changes in blood flow also influence the rate of delivery of drugs, which can be monitored with this instrument.

The effect of a "thermally significant vessel" on the response of the TDP system (in the transient mode) was examined in more detail in an isolated gracilis muscle preparation.[48] Multiple probes were inserted in the muscle, and total blood flow to the muscle was collected from venous return. Radioisotope labeled microspheres were used to assess regional variations in perfusion within the gracilis muscle as described above. $f(t)$ was determined by experiment to be $t^{-1/2}$. Figure 22 is a typical plot of probe power requirement ($V^2$ vs. $t^{-1/2}$) measured in the isolated gracilis muscle in the absence of a "thermally significant" vessel. Figure 23 is a typical plot of the probe power requirement when the thermistor was near a "thermally significant" vessel. The advancing thermal front, developed in the tissue by the heated probe, is detected to be in the vicinity of the "thermally significant" vessel at approximately 10 s. A typical comparison of calculated levels of perfusion determined with the TDP (in the presence of a "thermally significant" vessel) is shown in Fig. 24. Absolute flow calculations were made from data obtained using a 2–10 s regression "window" to determine the "infinite time" $V^2$ intercept. Typical variations in instantaneous values of measured perfusion were ±10%. Typical accuracy was within ±20%. The agreement of the short time, $k_{eff}$-derived flow with the independently measured, volume-averaged perfusion rate shows that perfusion can be quantified from data taken when a "thermally significant" vessel is present. It is interesting to note that the ±10% variation in instantaneous perfusion values (Fig. 24) corresponds to the mean variation observed when monitoring perfusion continuously (Fig. 19).

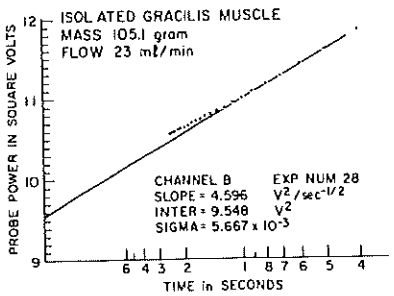


*FIGURE 23*
Typical plot of probe power vs. $t^{-1/2}$ when a "thermally significant" vessel is present.

*FIGURE 24*
Transient mode flow measur
determined from the simu
venous return in gracilis mus

## 13. COMPARISON W

The accuracy of t
more traditional therm
the rat liver preparatio
cold bolus of saline i
temperature response.
injected into the porta
resulting in a sudden c
drop and rate of cooli
the temperature of the l
are no spatial temperat
exponential time const
subsequent perfusion.

where $T$ is the liver t
specific heat of the pe
and $\alpha$ is the thermal
boundary conditions

Thus

Perfusion can be deter

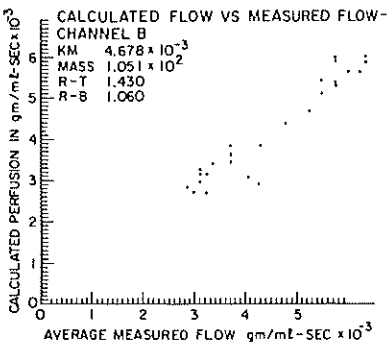


*FIGURE 24*
Transient mode flow measurements plotted vs. flows determined from the simultaneous collection of venous return in gracilis muscle.

## *13. COMPARISON WITH CAMERON'S METHOD*

The accuracy of the TDP system measurement in comparison with a more traditional thermal dilution method (Cameron, Ref. 16) was studied in the rat liver preparation. The latter technique consisted of the injection of a cold bolus of saline into the portal vein and monitoring the liver tissue temperature response. A bolus of 1–2 ml of saline at close to 0°C was quickly injected into the portal vein cannula, approximately 30 cm from the liver, resulting in a sudden cooling of the liver. The magnitude of the temperature drop and rate of cooling are proportional to the amount of bolus injected, the temperature of the bolus, and the rate of the injection. It is assumed there are no spatial temperature gradients within the region of the thermistor. The exponential time constant of the recovery phase is only dependent on the subsequent perfusion. The thermal model is simply

$$\frac{1}{\alpha}\frac{dT}{dt} = -\frac{\rho_b c_b w_b T}{k} \tag{42}$$

where $T$ is the liver tissue temperature, $w_b$ is the perfusion rate, $c_b$ is the specific heat of the perfusate, $k$ is the thermal conductivity of liver tissue, and $\alpha$ is the thermal diffusivity of liver tissue. Equation (42) is subject to boundary conditions

$$T = T_0 \qquad \text{at } t = 0 \tag{43}$$

$$T \to T_f \qquad \text{at } t \to \infty \tag{44}$$

Thus

$$T(t) = T_f - (T_f - T_0)e^{-zt} \tag{45}$$

Perfusion can be determined from the exponential time constant, $z$

$$w_b = \frac{kz}{\rho_b c_b \alpha} \tag{46}$$

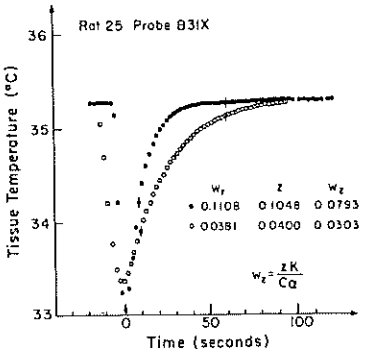


*FIGURE 25*
Transient temperature responses to a bolus injection of cold saline in the liver preparation. $w_r$ and $w_z$ are the perfusion rates determined by the thermal diffusion probe and Cameron methods, respectively.

Zero time is taken at the instant when the liver temperature is at a minimum. This minimum temperature is defined as the initial temperature, $T_0$. The final temperature can be taken as either the liver temperature before the bolus injection, or the liver temperature at 200 s. Two tissue temperature responses are displayed in Fig. 25. The only difference between the two experiments is the magnitude of the perfusion rate. Faster thermal recovery occurs at the higher perfusion rate. In this technique, the microsphere infusate served as the injected cold bolus, thus allowing simultaneous comparison of the two perfusion measurement techniques. Perfusion as measured by the cold bolus technique is plotted versus perfusion as measured by the radioactive microsphere technique in Fig. 26. Although the quantification by the thermal dilution technique was consistently low (slope = 0.751), the two measurements were well correlated ($\sigma_{xy} = 0.973$). The results show that the traditional thermal dilution or heat clearance method underestimates the perfusion rate. In contrast, the TDP system evaluated in the same rat liver model accurately predicted the perfusion rate.

## 14. SUMMARY

The experimental and clinical significance of regional blood flow warrants continued extensive efforts directed toward its quantification. Measure-

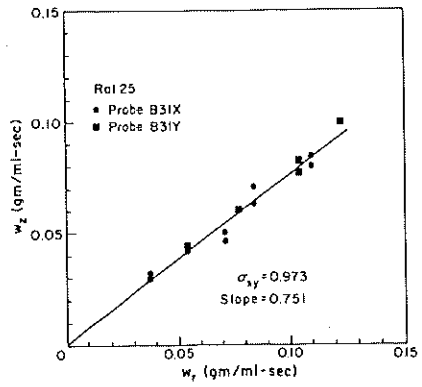


*FIGURE 26*
Cross plot of perfusion rates determined by the thermal diffusion probe ($w_r$) and Cameron methods ($w_z$) in the rat liver preparation.

ment techniques base
this regard because, in
be met.

Accurate measure
mally based technique
tions between the m
measured. The Therm
been singled out beca
evaluated of all of the
quantifying temperat
(intrinsic and effective
small volume measur
temporal and spatial
the data acquisition a

Several methods h
by heat clearance tec
have met with mixed s
cality in experimental
methods have been de
investigators must ulti
tions, some suggestion
fusion techniques.

Experiments shou
based on specific mod
of organ and tissue v
validity of the traditio
6) as well as recogniz
organization at the me
may be inconsistent w
heat balance: this may
clearance technique. S
ing. Microcirculatory
bed is not uniform in
properties of biologica
volumes constructed
effect of flexing, contr
rent heat exchange, su
requires detailed eval
in the dual capillary
Mixing of arterial flo
sinuses, and arterio-ve
examples requiring sp

Experiments sho
are compared with tho
ment. This would inc
that normalize the trar
method should be bas

ment techniques based on thermal clearance are particularly attractive in this regard because, in principle, all the necessary clinical requirements can be met.

Accurate measurement of thermal properties and perfusion using thermally based techniques requires a model that accounts for the thermal interactions between the measurement device and the medium (tissue) being measured. The Thermal Diffusion Probe (TDP) model and methodology has been singled out because it is currently the most highly developed and best evaluated of all of the thermal clearance techniques. It has the capability of quantifying temperature, thermal conductivity, and thermal diffusivity (intrinsic and effective) and perfusion. It has the advantages of a short time, small volume measurement, thereby minimizing problems associated with temporal and spatial variations in temperature and perfusion. Examples of the data acquisition and reduction protocols are included in this chapter.

Several methods have been developed for estimating regional blood flow by heat clearance techniques, as discussed in this chapter. These methods have met with mixed success when set against criteria of accuracy and practicality in experimental and clinical settings. Bearing in mind that improved methods have been developed recently for heat clearance technique, and that investigators must ultimately aim for clinical, as well as laboratory applications, some suggestions are offered for evaluating heat clearance based perfusion techniques.

Experiments should be designed to evaluated perfusion measurements, based on specific models of the heat clearance technique, covering the range of organ and tissue vasculature. These experiments should investigate the validity of the traditional assumptions of the bioheat transfer equation (Chap. 6) as well as recognize the dependence of the heat balance on local tissue organization at the measurement site (Chap. 7). The modeled thermal behavior may be inconsistent with reality, due to defects in these assumptions and the heat balance: this may in turn modify the prediction of perfusion by the heat clearance technique. Several examples of these defects are listed in the following. Microcirculatory flow is not a scalar quantity, and flow in any perfused bed is not uniform in time or space over small regions. The thermophysical properties of biological tissue are neither uniform nor isotropic. Tissue control volumes constructed for making heat balances usually do not include the effect of flexing, contracting, and moving tissue beds. The effect of countercurrent heat exchange, such as found in long, parallel arterial-venous vessel pairs, requires detailed evaluation. Regenerative heat exchange, such as may exist in the dual capillary circulation of the renal cortex, should be investigated. Mixing of arterial flows in the hepatic sinuses, complex flows in the splenic sinuses, and arterio-venous anastomoses in the cutaneous circulation are other examples requiring specific treatment and experimental evaluation.

Experiments should be carried out in which the heat clearance results are compared with those of an independent means of blood perfusion measurement. This would include other indicator dilution techniques, such as those that normalize the transfer function.[52] Preferably, the independent validation method should be based on other physical principles, such as the radioactive

microsphere uptake technique or venous collection. Isolated, thermally regulated organ systems in which total venous return and perfusate distribution can be independently measured appear to provide the most accurate evaluation of heat clearance techniques. Other methods, such as venous occlusion plethysmography and laser Doppler velocimetry have been applied to perfusion measurements. However, these methods have recognized, serious deficiencies for this application. Creative efforts to provide methods for perfusion measurement based on other sound physical principles are desirable.

The role of the invasive heat clearance measurement of perfusion should be put in context. Heat clearance measurement of blood flow must often be combined with measurements of species concentration, for example ATP, $p_{O_2}$, hydrogen ion, etc. Material balances are constructed from the combination of species concentration difference and flow data in order to evaluate normal or pathophysiological function or the effects of therapy. Thus, the perfusion measurement provides only part of the necessary data to achieve the end result, which is often an assessment of metabolic function. The heat clearance measurement must therefore meet appropriate criteria for evaluation of that function. Typical requirements for experimental or clinical evaluation of metabolic function include invasiveness, reliability, sensitivity, and practicality. Sensitivity analysis, a well-known engineering analytical technique, can be profitably employed to provide rational answers to some of these questions (Chap. 15).

The advent of microprocessing technology on a widely distributed basis makes it possible to evaluate the relative merits of many differing thermally based techniques. Of particular promise are those that can be broadly characterized as bolus, pulse-decay, periodic excitation, NMR, and other noninvasive approaches. Each technique has its advantages and disadvantages. It may well be that no one technique will be able to satisfy all clinical and investigative needs, and that ultimately, several techniques will need to be perfected. This story has not yet been written.

## *REFERENCES*


1. Kety, S. S. The theory and applications of the exchange of inert gas at the lungs and tissues. *Pharmacol. Rev.* 3, 1–41, 1951.
2. Wood, E. H. Symposium on use of indicator distribution technique in the study of the circulation. *Circulation Res.* 10, 357–581, 1961.
3. Bassingthwaighte, J. B. Blood flow and diffusion through mammalian organs. *Science* 167 (3923), 1347–1353, 1970.
4. Paradise, N. F., and Fox, I. J. Regional blood flow measurement. In: *Dye Curves: the Theory and Practice of Indicator Dilution*, D. A. Bloomfield, Ed., University Park Press, Baltimore, 1974, pp. 335–362.
5. Lassen, N. A. On the theory of the local clearance method for measurement of blood flow including a discussion of its application to various tissues. *Acta Med. Scandinavia Suppl.* 472, 136–145, 1967.
6. Koyama, T. Local myocardial blood flow measured by the use of a needle-type Pt–$H_2$ electrode. In: *Recent Advances in Studies on Cardiac Structure and Metabolism: The Metabolism of Contraction*, P. E. Roy, and G. Rona, Eds., University Park Press, Baltimore, 1975, Vol. 10, pp. 525–538.
7. Perl, W. Heat and matte
flow by local clearance
8. Rudolph, A. M, and He
distributions of blood
163–184, 1967.
9. Gibbs, F. A. A thermoe
*Med.* 31, 141–146, 193
10. Chen, M. M., and Hol
"Thermal Characteristi
*Acad. Sci.* 335, 137–15
11. Pennes, H. H. Analysis
*J. Appl. Physiol.* 1, 93–
12. Bowman, H. F. The bi
vessels. (In "Thermal C
*Ann. N.Y. Acad. Sci.* 3
13. Bowman, H. F., Crava
thermal properties of b
14. Bowman, H. F. Heat
(Third International Sy
Colorado State Univer
Monograph 61, Vol. 6
15. Tuttle, E. P., and Sadl
washout technique. In:
Texas, pp. 3–16.
16. Cameron. B. D. Determ
technique. *Phys. Med.*
17. Valvano, J. W., Allen,
conductivity, thermal
106 (3), 192–197, Aug
18. Eberhart, R. C., Jacks
determine regional blo
19. Hernandex, E. J., *et a*
generation. *Am. J. Phy*
20. Mitchell, J. W., *et al.*
859–865, 1970.
21. Cary, J., Mikic, B., an
Presented at 1973 W
Michigan, November
22. Shitzer, A. Comparisor
profiles inside the thig
23. Stow, R. W., and Sche
tissues in man. *J. App.*
24. Perl, W., and Hirsch, R
*J. Theoret. Biol.* 10, 2
25. Johnson, W. R., Abdel
analysis of the heated
99(*K*), 58–65, 1979.
26. Elkowitz, A. B., Shitz
with non-uniform bl
1982.
27. Muller-Schauenburg,
blood flow with heat
28. Bowman, H. F., Balas
from in vivo thermal
Annual Meeting, Uni
29. Chen, M. M., and Hol
of thermal conductivi

7. Perl, W. Heat and matter distribution in body tissues and the determination of tissue blood flow by local clearance methods. *J. Theoret. Biol.* **2**, 201–235, 1962.
8. Rudolph, A. M, and Heymann, M. A. Circulation of the fetus in utero; Methods for studying distributions of blood flow, cardiac output and organ blood flow. *Circulation Res.* **21**, 163–184, 1967.
9. Gibbs, F. A. A thermoelectric blood flow recorder in the form of a needle. *Proc. Soc. Exp. Med.* **31**, 141–146, 1933.
10. Chen, M. M., and Holmes, K. R. Microvascular contributions in tissue heat transfer. (In "Thermal Characteristics of Tumors: Applications in Detection and Treatment.") *Ann. N.Y. Acad. Sci.* **335**, 137–150, 1980.
11. Pennes, H. H. Analysis of tissue and arterial blood temperature in the resting human forearm. *J. Appl. Physiol.* **1**, 93–122, 1948.
12. Bowman, H. F. The bio-heat transfer equation and discrimination of thermally significant vessels. (In "Thermal Characteristics of Tumors: Applications in Detection and Treatment.") *Ann. N.Y. Acad. Sci.* **335**, 155–160, 1980.
13. Bowman, H. F., Cravalho, E.G., and Woods, M. Theory, measurement and application of thermal properties of biomaterials. *Ann. Rev. Biophys. Bioeng.* **4**, 43–80, 1975.
14. Bowman, H. F. Heat transfer mechanisms and thermal dosimetry. Invited review paper (Third International Symposium on Cancer Therapy by Hyperthermia, Drugs, and Radiation, Colorado State University, Ft. Collins, Colorado, June 22–26, 1980), *J. Nat. Cancer Inst.*, Monograph 61, Vol. 60, 1981, pp. 437–445.
15. Tuttle, E. P., and Sadler, J. H. Measurement of renal tissue fluid turnover rates by thermal washout technique. In: *Hypertension.* Monograph, 1965, American Heart Association, Dallas, Texas, pp. 3–16.
16. Cameron. B. D. Determination of regional cerebral cortical blood flow using a heat clearance technique. *Phys. Med. Biol.* **15**, 715–721, 1970.
17. Valvano, J. W., Allen, J. T., and Bowman, H. F. The simultaneous measurement of thermal conductivity, thermal diffusivity, and perfusion in small volumes of tissue. *J. Biomech. Eng.* **106** (3), 192–197, August 1984.
18. Eberhart, R. C., Jackson, M., and Trezek, G. J. Application of a heat transfer model to determine regional blood flow rate. *J. Heat Transfer* **95**(C), 113–119, 1973.
19. Hernandex, E. J., *et al.* Thermal quantification of regional myocardial perfusion and heat generation. *Am. J. Physiol.* **236**, H345–H355, 1979.
20. Mitchell, J. W., *et al.* Thermal response of human legs during cooling. *J. Appl. Physiol.* **29**, 859–865, 1970.
21. Cary, J., Mikic, B., and Johnson, R. Thermal methods for blood perfusion measurements. Presented at 1973 Winter Annual ASME Meeting, Bioengineering Division, Detroit, Michigan, November 11–15, 1973.
22. Shitzer, A. Comparison of analytically predicted and experimentally measured temperature profiles inside the thigh muscle of exercising men. *Math. Biosci.* **36**, 31–43, 1977.
23. Stow, R. W., and Scheive, J. F. Measurement of blood flow in minute volumes of specific tissues in man. *J. Appl. Physiol.* **14**, 215–224, 1959.
24. Perl, W., and Hirsch, R. L. Local blood flow in kidney tissue by heat clearance measurement. *J. Theoret. Biol.* **10**, 251–280, 1966.
25. Johnson, W. R., Abdelmessih, A. H., and Grayson, J. Blood perfusion measurements by the analysis of the heated thermocouple probe's temperature transients. *J. Biomech. Eng. ASME* **99**(*K*), 58–65, 1979.
26. Elkowitz, A. B., Shitzer, A., and Eberhart, R. C. Transient temperature profiles in tissues with non-uniform blood flow distributions. *J. Biomech. Eng. ASME* **104**(K), 202–208, 1982.
27. Muller-Schauenburg, W., Apfel, H., Benzing, H., Betz, E. Quantitative measurement of local blood flow with heat clearance. *Basic Res. Cardiol.* **70**, 547–567, 1975.
28. Bowman, H. F., Balasubramaniam, T. A., and Woods, M. Determination of tissue perfusion from in vivo thermal conductivity measurements. Paper No. 77-WA/HT-40, ASME Winter Annual Meeting, United Engineering Center, New York.
29. Chen, M. M., and Holmes, K. R. Thermal pulse-decay method for simultaneous measurement of thermal conductivity and local blood perfusion rate of living tissues. *1980 Advances in*

*Bioengineering*, V. C. Mow, Ed., ASME Winter Annual Meeting, United Engineering Center, New York, pp. 113–115.
30. Patera, A. T., Eden, G., Mikic, B. B., and Bowman, H. F. Prediction of tissue thermal properties from measurement of the phase shift between heat flux and temperature. *Adv. Biomed. Eng.*, M. K. Wells, Ed., ASME Winter Meeting, New York, 1979, p. 187.
31. Eden, G., and Bowman, H. F. Determination of tissue thermal conductivity, diffusivity, and perfusion from the phase-frequency response of a spherical heat source. Invited paper presented at the 1981 Annual Meeting of the Association for the Advancement of Medical Instrumentation (AAMI), Washington, D.C., May 10–14, 1981.
32. Bowman, H. F., and Walsh, J. T. Unpublished data, 1981–1983 (in preparation).
33. Walsh, J. T., and Bowman, H. F. Non-invasive measurement of thermal properties and perfusion. Presented at 35th Annual Conference on Engineering in Medicine and Biology, September 22, 1982, Philadelphia, Pennsylvania, vol. 24, p. 36.
34. Hensel, H. Fortlaufende Warmeleitfahigkeits- und Durchblutungsmessung im Gewebe mit einer Differential-Calorimetersonde. *Ber. Ges. Physiol.* 162, 360, 1953/54.
35. Golenhofen, K., and Hildebrandt, G. The method of heat conduction measurement and its importance for the physiology of human muscle blood circulation. *Arch. Kreislaufforsch.* 38, 23–70, 1962.
36. Betz, E., and Benzing, H. Continuous registration of local myocardial blood circulation on non-anesthetized un-restrained cats. *Dtsch. Ges. Kreislaufforsch.* 28, 437–440, 1963.
37. Hensel, H. Messkopf zur Durchblutungsregistrierung an Oberflachen. *Pflugers Arch. Gesamte Physiol.* 268, 604–606, 1958/59.
38. Betz, E., Hensel, H., and Du Mesnil de Rochemont, W. Simultane Messungen der lokalen Myokarddurchblutung mit Warmeleitmessungen und Krypton Clearance. *Pflugers Arch. Gesamte Physiol.* 288, 389–400, 1966.
39. Selkurt, E. E. The renal circulation. In: *Handbook of Physiology: Circulation*, Vol. II, W. F. Hamilton, Ed., American Physiological Society, Washington, D.C., 1963, pp. 1457–1516.
40. Chato, J. C. A method for the measurement of the thermal properties of biological materials. Thermal Problems in Biotechnology, Symposium Series, ASME, 1968, pp. 16–25.
41. Balasubramaniam, T. A., and Bowman, H. F. Thermal conductivity and thermal diffusivity of biomaterials: A simultaneous measurement technique. *J. Biomech. Eng. ASME* 99(*K*), 148–154, 1977.
42. Balasubramaniam, T. A., and Bowman, H. F. Temperature field due to a time dependent heat source of spherical geometry in an infinite medium. *J. Heat Transfer, ASME* 97(*C*), 296–299, 1974.
43. Bowman, H. F., and Balasubramaniam, T. A. A new technique utilizing thermistor probes for the measurement of thermal properties of biomaterials. *Cryobiology* 13(4), 572–580, 1976.
44. Balasubramaniam, T. A. Thermal conductivity and thermal diffusivity of biomaterials: A simultaneous single measurement technique. Ph. D. thesis in Mechanical Engineering. Northeastern University, June 1975.
45. Valvano, J. W. The use of thermal diffusivity to quantify tissue perfusion. Ph.D. thesis in Medical Engineering, Harvard–MIT Division of Health Sciences and Technology, June 1981.
46. Valvano, J. W., and Bowman, H. F. Transient temperature field in perfused tissue due to a self-heated thermistor. in preparation.
47. Valvano, J. W., Allen, J. T., Walsh, J. T., Hnatowich, D. J., Tomera, J. F., Brunengraber, H., and Bowman, H. F. An isolated rat liver model system for the evaluation of thermal techniques to quantify perfusion. *J. Biomech. Eng.* 106 (3), 187–191, August 1984.
48. Woods, M., and Bowman, H. F. Unpublished data.
49. Bowman, H. F., Hernandez, E. J., Valvano, J. W., and Siegel, J. H. Unpublished data.
50. Brunengraber, H., Boutry, J., and Lowenstein, J. M. Fatty acid and 3-$\beta$-hydroxysterol synthesis in the perfused rat liver. *J. Biol. Chem.* 248(8), 2656–2669, April 1973.
51. Bishop, S. P. Radioactive tracer microspheres: Practical considerations to determine regional organ blood flow in experimental animals. *Med. Electron.* 66–73, June 1981.
52. Bassingthwaighte, J. B. Blood flow and diffusion through mammalian organs. *Science* 167, 1347–1353, 1970.
53. Chen, M. M., Holmes, K. R., and Rupinskas, V. Pulse-decay method for measuring the thermal conductivity of living tissues. *J. Biomech. Eng.* 103, 253, 1981.

# *GENERAL BIOHEAT*

*Avraham Shitze*

## *1. INTRODUCTION*

The analysis of th
may be multifaceted,
quite obvious and is tr
the existence and relati
in boundary and initi
possibility of developi
thermal behavior of bi

Nevertheless, certa
energy balance in as g
of the need to solve a
observe, in a general w
behavior of the tissue,
the relationships whic

A few attempts ha
All of these studies tre
or no consideration is
to the overall behavio
other studies (c.f. Cha

In 1972 Lin atte
general problem relati
account for heat trans
graphical illustrations
no physical conclusio
as a general analysis of
tions to biological tiss

Shitzer and Kleine
in 1975.[4] In their w
principle represents t
energy balance. This

*Avraham Shitzer* • Dep
Technology, Haifa, Israel.